Dynamic modeling and in-plane 1:1:1 internal resonance analysis of cable-stayed bridge

Hou Jun Kang[1], Tie Ding Guo[1], Yue Yu Zhao[1], Wen Bin Fu[2]

1. College of Civil Engineering, Hunan University, Changsha 410082, Hunan, People's Republic of China
2. College of Mechanical and Vehicle Engineering, Hunan University, Changsha 410082, Hunan, People's Republic of China

Abstract:

A novel nonlinear dynamic double-cable-stayed shallow-arch model of cable-stayed bridge is established and the in-plane 1:1:1 internal resonance between three first modes of shallow arch and two cables under both external primary and subharmonic resonance is investigated, respectively. The Galerkin discretization and the method of multiple scales are applied to obtain the modulation equations of the dynamic system. The stable equilibrium solutions of the modulation equations are examined by direct integration i.e. Runge-kutta method. Numerical simulations are carried out to investigate the dynamic behavior of the new dynamic system. The results show the rich nonlinear phenomena and some new conclusions are drawn.

Keywords: modeling;nonlinear;dynamics;cable-stayed bridge.

1. Introduction

In the past few decades, cable-stayed bridges became very popular especially when designed to cross valleys, wide rivers and even strait, which is a consequence of their inherent mechanical effectiveness, economical design, and esthetic appearance. Although high performance materials are used to increase these structures' stiffness, such structures are very flexible and light and become very sensitive to traffic, wind, rain-wind and earthquake induced vibrations. Thus, stay cables and global cable-stayed bridges are prone to vibrate locally or globally. Therefore, exploration of the dynamic behavior of these structures under time-varying loads has become an important research area. Research on dynamics of cable-stayed bridges went through two stages in the past decades. One is the dynamics of single member with ideal excitations such as cable and beam, and the other is the dynamics of hybrid structure with internal resonance such as cable-beam.

Cable dynamics has a long and rich history documented in the classic monograph by Irvine (Irvine,1981), and summarized in the review articles by Triantafyllou (Triantafyllou,1991), Starossek (Starossek,1994) and Rega (Rega, 2003a,2003b). Based on the parabolic static equilibrium configuration, linear free and forced oscillations of elastic cables with small sag were first developed by Irvine and Caughey (Irvine,1981). Based on a single-degree-of-freedom model for in-plane vibrations of a cable, Hagedorn and Shafer (Hagedorn and Schafer, 1980) extended the linear theory considering the effect of quadratic and cubic non-linearities on eigen frequencies.

Cubic non-linearities due to cable stretching and quadratic non-linearities due to equilibrium cable curvature couple these motion components in producing full three-dimensional cable response, namely modal interaction. A two-degree-of-freedom approximation of the model was developed by Perkins (Perkins, 1992), which described a class of in-plane/out-of-plane motions that are coupled through the quadratic non-linearities. Thereafter, many studies have focused on the modal interaction between in-plane and/or out-of-plane motions (Zhao and Wang, 2006; Pilipchuk and Ibrahim, 1997, 1999; Arafat and Nayfeh, 2003)and even between longitudinal and transversal motions(Srinil and Rega, 2008). With the extension of main span of cable-stayed bridge the effect of bending stiffness in these large-diameter bridge cables is not negligible. An investigation on accurate finite element modeling of large-diameter sagged cables taking into account flexural rigidity and sag extensibility was carried out by Ni et al(Ni et al.,2002). With consideration of flexural rigidity and sag extensibility the three-to-one internal resonance between the first- and third-order in-plane symmetrical modes is analyzed by Kang et al.(Kang et al.,2015).

There also have been many attempts to understand the dynamic interactions between the stay cables and the structural components such as the bridge deck and the towers. From an engineering viewpoint, Gimsing (Gimsing and Georgakis,1983) classified vibrations of cable-stayed bridges into two types, namely 'local' vibrations and 'global' vibrations. Cable vibrations are local, in the sense that the anchorage points at girder and pylon are fixed. On the other hand, girder-pylon vibrations are global, since the whole bridge span vibrates. Warnitchai et al. (Warnitchai et al., 1995). separated the cable motions into two parts: the quasi-static motions and the modal motions. The quasi-static motions are the displacements of the cables that move as an elastic tendon with the supports, and the modal motions are the vibrations of the cables with fixed ends. However, to get for the quasi-static motions of the cables, the mode shapes of the bridge deck and the towers are separately obtained from the conventional finite element analysis. To avoid the limitation of the above approach, Gattulli and his co-workers (Gattulli et al., 2002) proposed the hybrid mode shapes of a family of linearized cable-stayed beam systems by solving the eigenvalue problem of an entire structure. Thereafter they (Gattulli and Lepidi, 2003) have revealed that some combinations of the system parameters can result in 1:1 internal resonance between the so-called local and global modes. Recently, following the methodologies in Refs(Gattulli and Lepidi, 2003), Cao et al. (Cao et al.,2012) proposed a cable-stayed bridge model that consists of a simply-supported four-cable-stayed deck beam and two rigid towers, aiming to understand the complex dynamic interactions between the cables and the deck beam.

Although the natural frequencies and mode shapes of cable-stayed bridges have been calculated by a cable model or a cable-beam model, or multiple cable and a deck beam model, and even internal resonances between cables and deck beam have been revealed, they often have difficulties in analyzing their nonlinear dynamic behavior under external excitation such as moving vehicle loading, rain/wind loading and earthquake loading. Additionally, in these studies, 1:1, 1:2 and 2:1 internal resonances (Gattulli and Lepidi, 2003; Wei et al., 2012,2014; Gattulli et al.,2005) between modes of cable and beam have been analytically and experimentally investigated, but it is more interesting to explore the internal resonances between modes of multiple cables and beam, such as 1:1:1 internal resonance and others between two cables and a beam, since that there always exists almost same frequencies of cables in cable-stayed bridges(Cao et al.,2012; Caetano et al., 2000; Ren et al., 2005). Then, it is very common that the initial static configurations of deck beam are designed in cable-stayed bridges and their effect on

nonlinear dynamics is neglected in previous works. Actually, it is also well-known that the initial static configurations of cable and shallow arch are very important to their dynamical properties. Hence, the initial static configuration of deck beam should be considered in nonlinear dynamic analysis of cable-stayed bridge. Therefore, it is interesting and meaningful to establish a new dynamic model of cable-stayed bridges, which may can predict some new dynamic phenomena and reveal their mechanism of this kind of bridge.

The objective of the present work is to develop a general dynamic model for understanding the complex dynamic interactions of cable-stayed bridge. The investigation begins with the development of a continuum model representing the cable-stayed bridge. Based on the classic dynamic theories of cables and shallow arch, a double-cable-stayed shallow arch mechanical model and its differential equations governing in-plane motion of cable-stayed bridge will be established. The double-cable-stayed shallow-arch model studied here is closer to a real cable-stayed bridge than those in the previous works, where it can be used to analyze the modal interaction not only between cable and deck but also between cables. Considering simultaneous external resonance and 1:1:1 internal resonance, a set of non-linear partial differential equations governing the motion of the dynamic model are solved by Galerkin method and the method of multiple scales perturbation. Finally, the nonlinear phenomena of a planar double-cable-stayed shallow-arch model for cable-stayed bridge are explored by means of numerical analysis.

2. Modeling and equations of in-plane motion

2.1 Modeling of cable-stayed bridge.

Fig. 1 shows the lateral view of general cable-stayed bridge, which is constructed commonly in the world. This kind of bridge is of the following feature. One of them is that the bending stiffness of tower is biggest than those of cables and deck. Hence, the tower is generally regarded as a stiff tower and cables and deck are flexible in most of references (Gattulli et al., 2002, 2005; Gattulli and Lepidi, 2003,2007; Cao et al.,2012) Another is that the cables are arranged densely, which leads to that the fundamental frequencies of cables are dense (Ren et al., 2005) and that 1:1, 2:1 and 1:2 between frequencies of cable and deck are commonly(Gattulli and Lepidi, 2003; Wei et al., 2012,2014; Gattulli et al.,2005). Generally, the mode shapes of deck can be illustrated by sine functions(Chang et al.,2001; Bruno and Leonardi,1997), especially for floating deck. For brevity, the mode shapes of shallow arch are assumed to be sine functions as shown in section 4.2. Fig. 2 shows the modal shape and dynamic model of cable-stayed bridge with two towers. Especially, Fig. 2(a) and (b) were obtained by finite element method (Abdel-Ghaffar and Khalifa,1991) and Fig. 2(c) was obtained by analytical method (Cao et al.,2012). Based on these work, the cable-beam model is proposed to study the interaction between cable and deck. Although some of the dynamic properties of cable-stayed bridge have been revealed and the geometry boundary conditions and mechanical ones between cable and beam have been discussed in many references, the model itself has many shortcomings. For example, the internal bending moment of the cross section of beam is generally not zero at the anchored point, which is apparently different from the geometry boundary conditions and mechanical ones at the anchored point of the cable-supported cantilever beam. Actually, the cable-supported cantilever beam exists only in the construction stage of cable-stayed bridge. Therefore, the cable-beam model is only applicable to the construction stage of cable-stayed bridge. For the working bridge, actually there is no cable-supported cantilever beam as shown in Fig. 1. Thus, based on these researches the

double-cable-stayed shallow arch model as shown in Fig. 3, is proposed to study the nonlinear dynamics of general cable-stayed bridge.

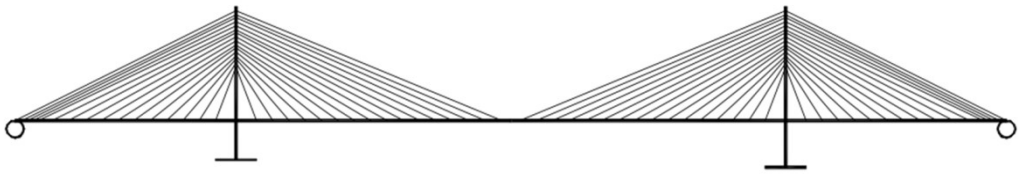

Fig.1 Lateral view of general cable-stayed bridge

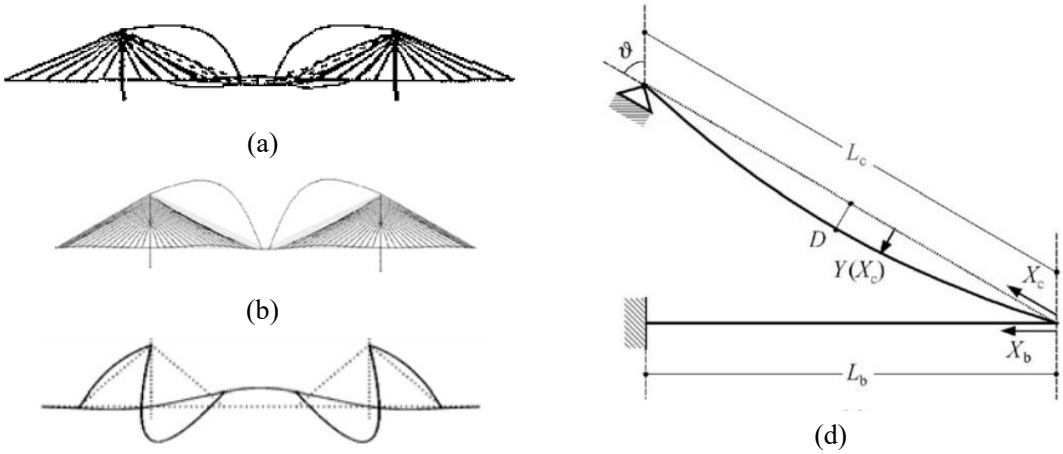

Fig. 2 modal shape and cable-beam model of general cable-stayed bridge: (a), (b) and (c) are modal shape and (d) is a dynamic model.

The double-cable-stayed shallow-arch model consists of a simply-supported and cable-stayed shallow arch and two cables, as shown in Fig. 3. Two cables are used to illustrate the possible internal resonance between cables and deck, where the other cables are assumed to be static. That is, frequencies of others do not match with those of deck. The other static cable, which is assumed not to vibrate, plays a role of elastic support to deck. Their contribution of elastic support on deck is considered by increasing stiffness of shallow arch. It should also be illustrated that the towers of cable-stayed bridge are assumed to be rigid due to the fact that experimental measurements on and finite element analysis of a real cable-stayed bridge demonstrate that the towers have minimal vibrations (Cao et al.,2012; Caetano et al.,2008). Hence, the two cables are assumed to be clamped at upper ends (Wei et al., 2014) and the lower ends are anchored at the junctions s_1, s_2. To simplify the calculation, we now assume that the axial strain of shallow arch does not depend on s but the transverse deflection w (Mettler, 1962). The ratio ($h_a = 2f_a / L$) of rise to span of the shallow arch is very small, which is less than 0.03. It is known that there are many kinds of loads acting on the bridge. In this paper, our attention is focused on the axial motion of the right end of shallow arch, which can be induced through expansion joints by vehicle or seismic load. Although the shallow arch is of elastic extensibility in axial direction, only the right end load is considered since that the vertical deflection of deck is usually greater than that of axial direction. Therefore, the effect of cable vibration on axial deformation of shallow arch is neglected. The

effect of cable vibration on vertical deformation of shallow arch is considered as an external load as shown in Eq. (3). On the other hand, the effects of motion of shallow arch on cable are assumed to be vertical excitation at the lower end.

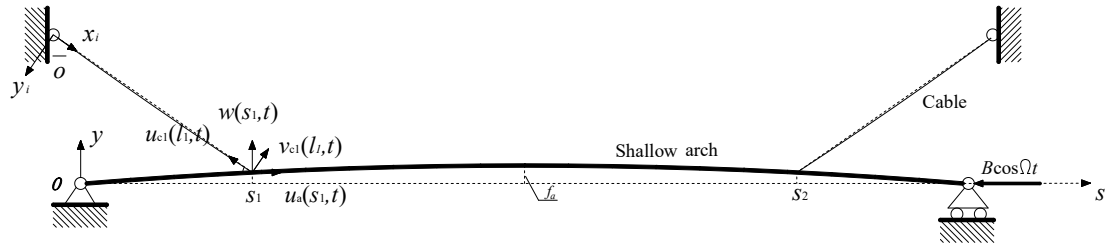

Fig. 3 Double-cable-stayed shallow-arch model of cable-stayed bridge

The equation (Malhotra and Namachchivaya,1997) of motion governing the lateral deflection $w_a(s,t)$ of shallow arch, subjected to a lateral loading $p_a(s,t)$, can be derived by using the energy method and is given as

$$EIw''''-EAh(w,t)\left(w''+y''\right)+\mu\dot{w}+\rho A\ddot{w}=p(s,t) \tag{1}$$

$$h(w,t)=\frac{1}{L}\left[u(L,t)+\int_0^L\left(\frac{1}{2}w'^2+y'w'\right)\mathrm{d}s\right] \tag{2}$$

where, ρ, E, I, μ and A are density per unit length, Young's modulus, moment of inertia, damping parameter and cross-section area of shallow arch, respectively. y is the initial deflection of the unloaded shallow arch. L is the span of shallow arch. In Eqs. (1) and (2), the subscript *a* denotes the shallow arch, and apex and dot denotes differentiation with respect to the abscissa s and the time t.

The shallow arch is assumed to be subjected to a lateral loading $p(s,t)$ induced by two cables and to an axial load $u(L,t)$ induced by end excitation. Here, the lateral and axial loading can be written as

$$p_a(s,t)=\sum_{j=1}^{2}\delta(s-s_j)\frac{E_jA_j}{l_j}e_j(t)\sin\theta_i \tag{3}$$

$$u(L,t)=B\cos(\Omega t) \tag{4}$$

where, $\delta(s-s_1)$ is Dirac delta function, θ denotes the inclined angle of cable, namely the acute angle between the horizontal line and axis x_i of cables, as shown in Fig. 3, B and Ω denote the external excitation amplitude and frequency, respectively. The subscripts a and c are abbreviation of arch and cable, severally. It needs to be noted that the angle between the tangential line of shallow arch and horizontal line is neglected in derivation of Eq. (3) since that the initial deflection of shallow arch is very small.

Under the previous assumptions and by using the classical extended Hamilton's principle and the standard condensation procedure (Luongo, 1984), the equations of cables' motion governing the in-plane transverse vibration are obtained (Gattulli et al.,2002)

$$\rho_j A_j \ddot{v}_j + \mu_j \dot{v}_j - \left[H_j v_j' + E_j A_j \left(y_j' + v_j' \right) e_j(t) \right]' = p_j(x_j, t) \ (j = 1, 2) \tag{5}$$

where, $e_t(t)$ represents the uniform dynamic elongation given by

$$e_j(t) = -\frac{w(s_j, t)}{l_j} \sin\theta_j + \frac{1}{l_j} \int_0^{l_j} \left(y_j' v_j' + \frac{1}{2} v_j'^2 \right) \mathrm{d}x_j \qquad (j = 1, 2) \tag{6}$$

In Eqs. (5) and (6) apex and dot denotes differentiation with respect to the abscissa x_j and the time t. E_j, A_j, p_j and H_j are the Young's modulus, area of cross section, load per unit length and horizontal component of the initial tension of the j th cable.

Till now, the partial differential equations governing motion of double-cable-stayed shallow-arch model have been established as shown in Eqs. (1) to (6). It needs to be noted that the in-plane transversely forced excitation at the lower end of cable induced by in-plane transverse motion of shallow arch is considered in transverse displacements of cable. It is well-known that the existence of both types of modes in transverse displacements are described as the cable being quasi-statically dragged by the shallow arch as global modes and modes localized in the cable domain known as local modes(Wei et al.,2014; Warnitchai et al.,1995; Wu et al., 2003). Therefore, based on the study in these works, the in-plane transverse displacements v_1 and v_1 are approximated as follows:

$$v_1(x_1, t) = w\left(s_1, t\right) x_1 \cos\theta_1 + \varphi_1(x_1) q_1(t) \tag{7}$$

$$v_2(x_2, t) = w\left(s_2, t\right) x_2 \cos\theta_2 + \varphi_2(x_2) q_2(t) \tag{8}$$

where,

$$w(s, t) = \phi(s) g(t) \tag{9}$$

Owing to the definition of the lateral loads in Equation (3), the elongation in Equation (6) and the transverse displacements in Eqs. (7) and (8) of cables, problem (1) and (5), in addition to the well-known quadratic and cubic interaction terms of both cable and shallow arch, shows the existence of coupling terms between the double-cable-stayed shallow-arch dynamics.

Considering Eqs. (3) and (4), a non-dimensional form of problem (1) and (5) can be obtained by introducing the following variables:

$$x_j^* = \frac{x_j}{l_j}, \tau = \omega_1 t, y_j^* = \frac{y_j}{l_j}, v_j^* = \frac{v_j}{l_j}, \mu_j^* = \frac{\mu_j}{\rho_j A_j \omega_1}, \lambda_j^* = \frac{E_j A_j}{H_j}, \beta_j^2 = \frac{\rho_j A_j l_j^{\,2} \omega_1^2}{H_j}, w^* = \frac{w}{L},$$

$$\gamma_j = \frac{L}{l_j}, s^* = \frac{s}{L}, y = \frac{y_a}{L}, \mu^* = \frac{\mu}{\rho A \omega_1}, B^* = \frac{B}{L}, \Omega^* = \frac{\Omega}{\omega_1}, K_j = \frac{E_j A_j}{\rho A \omega_1^2 L l_j}, \beta^4 = \frac{\rho A \omega_1^2 L^4}{EI},$$

$$\eta = \frac{AL^2}{I}. \tag{10}$$

where ω_1 is the natural frequency of the system in-plane. In the nondimensional form, Eqs.(1)–(2) and (5)-(6) become:

$$\frac{1}{\beta^4}w''''-\frac{\eta}{\beta^4}h(w,t)\left(w''+y''\right)+\mu\dot{w}+\ddot{w}=\sum_{j=1}^{2}\delta(s-s_j)K_j e_j(t)\sin\theta_j \tag{11}$$

$$h(w,t)=B\cos(\Omega t)+\int_0^1\left(\frac{1}{2}w'^2+y'w'\right)\mathrm{d}s \tag{12}$$

$$\ddot{v}_j+\mu_j\dot{v}_j-\frac{1}{\beta_j^2}\left[v_j''+\lambda_j\left(y_j''+v_j''\right)e_j(t)\right]=0 \tag{13}$$

$$e_j(t)=-\gamma_j w(s_j,t)\sin\theta_j+\int_0^1\left(y_j'v_j'+\frac{1}{2}v_j'^2\right)\mathrm{d}x_j \tag{14}$$

where the asterisks are dropped for simplicity. Similarly, Eqs. (7)-(9) can be rewritten in nondimensional form as

$$v_1(x_1,\tau)=w\left(s_1,\tau\right)x_1\cos\theta_1+\varphi_1(x_1)q_1(\tau) \tag{15}$$

$$v_2(x_2,\tau)=w\left(s_2,\tau\right)x_2\cos\theta_2+\varphi_2(x_2)q_2(\tau) \tag{16}$$

$$w(s,\tau)=\phi(s)g(\tau) \tag{17}$$

With these assumptions, the nonlinear governing equations of motion with three degrees-of-freedom for the double-cable-stayed shallow–arch coupled system can be derived by substituting (15)-(17) into (11)-(14) and implementing the Galerkin method(Ding and Chen,2010). This yields the following set of equations:

$$\ddot{g}+\mu\dot{g}+b_{11}g+b_{12}g\cos\Omega\tau+b_{13}g^2+b_{14}g^3+b_{15}q_1+b_{16}gq_1+b_{17}q_1^2+$$

$$b_{18}q_2+b_{19}gq_2+b_{110}q_2^2+b_{111}\cos\Omega\tau=0 \tag{18}$$

$$\ddot{q}_1+\mu_1\dot{q}_1+b_{21}\dot{g}+b_{22}\ddot{g}+b_{23}g+b_{24}g^2+b_{25}q_1+b_{26}gq_1+$$

$$b_{27}g^2q_1+b_{28}q_1^2+b_{29}gq_1^2+b_{210}q_1^3=0 \tag{19}$$

$$\ddot{q}_2+\mu_2\dot{q}_2+b_{31}\dot{g}+b_{32}\ddot{g}+b_{33}g+b_{34}g^2+b_{35}q_2+b_{36}gq_2+$$

$$b_{37}g^2q_2+b_{38}q_2^2+b_{39}gq_2^2+b_{310}q_2^3=0 \tag{20}$$

where b_{ij} $(i=1,2,3;\ j\le 11)$ are the Galerkin integral coefficients of the cables and shallow arch, respectively, which are reported in Appendix A. From Eq. (18), it is noted that the axial load at end of shallow arch can induce a parametric and force excitation. From Eqs. (18)-(19), we can see that the coupling between cable and shallow arch are complex and different from those in cable-beam system(Wei et al.,2012; Gattulli et al.,2005). Therefore, the nonlinear interaction

between cables and shallow arch and new phenomena are expected.

3. Perturbation analysis

In this section, the method of multiple scales (MMS) (Nayfeh and Mook,1979) is directly applied to the governing equations (18)-(20) for determining the steady-state responses. Firstly, we introduce a bookkeeping parameter ε, which is later set to 1, rescale the parameters of these governing equations including the damping coefficients and the external load.

The equations of motion governing the model of a double-cable-stayed shallow-arch coupled system in nondimensional form are rewritten as:

$$\ddot{g}+\varepsilon^2\mu\dot{g}+\omega_a^2 g+\varepsilon^2 b_{12}g\cos\Omega\tau+\varepsilon b_{13}g^2+\varepsilon^2 b_{14}g^3+\varepsilon b_{15}q_1+\varepsilon b_{16}gq_1+\varepsilon b_{17}q_1^2+$$

$$\varepsilon b_{18}q_2+\varepsilon b_{19}gq_2+\varepsilon b_{110}q_2^2+\varepsilon^2 b_{111}\cos\Omega\tau=0 \tag{21}$$

$$\ddot{q}_1+\varepsilon^2\mu_1\dot{q}_1+\varepsilon^2 b_{21}\dot{g}+\varepsilon^2 b_{22}\ddot{g}+\varepsilon b_{23}g+\varepsilon b_{24}g^2+\omega_b^2 q_1+\varepsilon b_{26}gq_1+$$

$$\varepsilon^2 b_{27}g^2q_1+\varepsilon b_{28}q_1^2+\varepsilon^2 b_{29}gq_1^2+\varepsilon^2 b_{210}q_1^3=0 \tag{22}$$

$$\ddot{q}_2+\varepsilon^2\mu_2\dot{q}_2+\varepsilon^2 b_{31}\dot{g}+\varepsilon^2 b_{32}\ddot{g}+\varepsilon b_{33}g+\varepsilon b_{34}g^2+\omega_c^2 q_2+\varepsilon b_{36}gq_2+$$

$$\varepsilon^2 b_{37}g^2q_2+\varepsilon b_{38}q_2^2+\varepsilon^2 b_{39}gq_2^2+\varepsilon^2 b_{310}q_2^3=0 \tag{23}$$

where $\omega_a^2=b_{11}, \omega_b^2=b_{25}, \omega_c^2=b_{35}$.

The displacements g and q_i are expanded as

$$g=\sum_{j=1}^{3}\varepsilon^{j-1}g_j(T_0,T_2)+O(\varepsilon^3), q_i=\sum_{j=1}^{3}\varepsilon^{j-1}q_{ij}(T_0,T_2)+O(\varepsilon^3), (j=1,2) \tag{24}$$

where, $T_0=\tau$, is the fast time scale associated with changes occurring at the frequencies ω_a, ω_b, ω_c and Ω, $T_2=\varepsilon^2\tau$ is the slow time scale associated with modulations in the amplitudes and phases caused by the nonlinearity, damping and resonances.

Substituting Eq. (24) into Eqs. (21)-(23), then equating the coefficients of the same powers of ε, we obtain the following differential equations:

$$\varepsilon^0:\ (D_0^2+\omega_a^2)g_1=0 \tag{25}$$

$$(D_0^2+\omega_b^2)q_{11}=0 \tag{26}$$

$$(D_0^2+\omega_c^2)q_{21}=0 \tag{27}$$

$$\varepsilon^1:\ (D_0^2+\omega_a^2)g_2=-b_{13}g_1^2-b_{15}q_{11}-b_{16}g_1q_{11}-b_{17}q_{11}^2-b_{18}q_{21}-b_{19}g_1q_{21}-b_{110}q_{21}^2 \tag{28}$$

$$(D_0^2+\omega_b^2)q_{12}=-b_{23}g_1-b_{24}g_1^2-b_{26}g_1q_{11}-b_{28}q_{11}^2 \tag{29}$$

$$(D_0^2+\omega_c^2)q_{22}=-b_{33}g_1-b_{34}g_1^2-b_{36}g_1q_{21}-b_{38}q_{21}^2 \tag{30}$$

$$\varepsilon^2:\ (D_0^2+\omega_a^2)g_3=-2D_0^1D_1^1g_1-\mu D_0^1g_1-b_{14}g_1^3-2b_{13}g_1g_2-b_{15}q_{12}-b_{16}g_2q_{11}-b_{16}g_1q_{12}-$$
$$2b_{17}q_{11}q_{12}-b_{18}q_{22}-b_{19}g_2q_{21}-b_{19}g_1q_{22}-2b_{110}q_{21}q_{22}-b_{111}\cos\Omega\tau-b_{12}g_1\cos\Omega\tau \tag{31}$$

$$(D_0^2+\omega_b^2)q_{13}=-2D_0^1D_1^1q_{11}-\mu_1D_0^1q_{11}-b_{21}D_0^1g_1-b_{22}D_0^2g_1-b_{23}g_2-2b_{24}g_1g_2-$$
$$b_{26}g_2q_{11}-b_{26}g_1q_{12}-b_{27}g_1^2q_{11}-2b_{28}q_{11}q_{12}-b_{29}g_1q_{11}^2-b_{210}q_{11}^3 \tag{32}$$

$$(D_0^2+\omega_c^2)q_{23}=-2D_0^1D_1^1q_{21}-\mu_2D_0^1q_{21}-b_{31}D_0^1g_1-b_{32}D_0^2g_1-b_{33}g_2-2b_{34}g_1g_2-$$
$$b_{36}g_2q_{21}-b_{36}g_1q_{22}-b_{37}g_1^2q_{21}-2b_{38}q_{21}q_{22}-b_{39}g_1q_{21}^2-b_{310}q_{21}^3 \tag{33}$$

where $D_j^m=\frac{\partial^m}{\partial T_j}, m=1,2$ and $j=0,2$.

The general solution of Eqs.(25) - (27) can be expressed as

$$g_1=A_1(T_2)\exp(i\omega_aT_0)+cc \tag{34}$$

$$q_{11}=A_2(T_2)\exp(i\omega_bT_0)+cc \tag{35}$$

$$q_{21}=A_3(T_2)\exp(i\omega_cT_0)+cc \tag{36}$$

where $A_j(T_2), j=1,2,3$, are complex functions in T_2, which are defined in the next section (cc denotes a complex conjugate of the preceding term). Substituting Eqs.(34) - (36) into Eqs. (28) - (30), we get

$$g_2=\frac{b_{13}}{3\omega_a^2}A_1^2\exp(2i\omega_aT_0)-\frac{b_{15}A_2\exp(i\omega_bT_0)}{\omega_a^2-\omega_b^2}+\frac{b_{16}A_1A_2\exp(i(\omega_a+\omega_b)T_0)}{\omega_b(2\omega_a+\omega_b)}-$$
$$\frac{b_{17}A_2^2\exp(2i\omega_bT_0)}{\omega_a^2-4\omega_b^2}+\frac{b_{18}A_3\exp(i\omega_cT_0)}{\omega_c^2-\omega_a^2}+\frac{b_{19}A_1A_3\exp(i(\omega_a+\omega_c)T_0)}{\omega_c(2\omega_a+\omega_c)}-$$
$$\frac{b_{110}A_3^2\exp(2i\omega_cT_0)}{\omega_a^2-4\omega_c^2}-\frac{b_{16}A_1B_2\exp(i(\omega_a-\omega_b)T_0)}{\omega_b(2\omega_a-\omega_b)}-\frac{b_{19}A_1B_3\exp(i(\omega_a-\omega_c)T_0)}{\omega_c(2\omega_a-\omega_c)}-$$
$$\frac{b_{13}A_1B_1}{\omega_a^2}-\frac{b_{17}A_2B_2}{\omega_a^2}-\frac{b_{110}A_3B_3}{\omega_a^2}+cc \tag{37}$$

$$q_{12}=\frac{b_{23}A_1\exp(i\omega_aT_0)}{\omega_a^2-\omega_b^2}+\frac{b_{24}A_1^2\exp(2i\omega_aT_0)}{4\omega_a^2-\omega_b^2}+\frac{b_{26}A_1A_2\exp(i(\omega_a+\omega_b)T_0)}{\omega_a(2\omega_b+\omega_a)}+$$

$$\frac{b_{28}A_2^2\exp(2i\omega_b T_0)}{3\omega_b^2}+\frac{b_{26}A_1B_2\exp(i(\omega_a-\omega_b)T_0)}{\omega_a(\omega_a-2\omega_b)}-\frac{b_{24}}{\omega_b^2}A_1B_1-\frac{b_{28}}{\omega_b^2}A_2B_2+cc \tag{38}$$

$$q_{22}=\frac{b_{33}A_1\exp(i\omega_a T_0)}{\omega_a^2-\omega_c^2}+\frac{b_{34}A_1^2\exp(2i\omega_a T_0)}{4\omega_a^2-\omega_c^2}+\frac{b_{36}A_1A_3\exp(i(\omega_a+\omega_c)T_0)}{\omega_a(2\omega_c+\omega_a)}+$$

$$\frac{b_{38}A_3^2\exp(2i\omega_c T_0)}{3\omega_c^2}+\frac{b_{36}A_1B_3\exp(i(\omega_a-\omega_c)T_0)}{\omega_a(\omega_a-2\omega_c)}-\frac{b_{34}}{\omega_c^2}A_1B_1-\frac{b_{38}}{\omega_c^2}A_3B_3+cc \tag{39}$$

where $B_j(T_2)$, $j=1,2,3$, are the corresponding complex conjugates of $A_j(T_2)$. In these work on cable-beam system, the response to external harmonic excitation of the global mode has been used to demonstrate the global–local interaction. Thus, the distances to the internal and external resonant conditions have been appropriately described through the relations

$$\omega_b=\omega_a+\varepsilon^2\sigma_2,\qquad \omega_c=\omega_a+\varepsilon^2\sigma_3 \tag{40}$$

wherer σ_2 and σ_3 describe the internal detuning parameters between frequencies of cables and shallow arch. Note that the detuning parameter of the forcing frequency is not introduced here and will be introduced later. The main cause is that the primary and subharmonic resonance of the global mode namely, the first mode of shallow arch, will be considered respectively.

Substituting the zero and first-order solutions in Eqs. (34)-(39) and Eq. (40) into the third-order perturbation equations in Eqs. (31)-(33), we obtain the third-order in-plane equations

$$\begin{aligned}(D_0^2+\omega_a^2)g_3=&-\tfrac{1}{2}b_{111}\exp(i\Omega T_0)-\tfrac{1}{2}b_{12}\exp(i(\Omega-\omega_a)T_0)-i\omega_a(\mu A_1+2A_1')\exp(i\omega_a T_0)+\\&\left(\Gamma_1^{\mathrm{a}}A_1+\Gamma_2^{\mathrm{a}}A_1^2B_1+\Gamma_{11}^{\mathrm{a}}A_1A_2B_2+(\Gamma_{15}^{\mathrm{a}}+\Gamma_{18}^{\mathrm{a}})A_1A_3B_3\right)\exp(i\omega_a T_0)+\\&(\Gamma_4^{\mathrm{a}}A_1A_2B_1+\Gamma_{12}^{\mathrm{a}}A_2^2B_2+\Gamma_{16}^{\mathrm{a}}A_2A_3B_3)\exp(i\omega_b T_0)+\\&(\Gamma_6^{\mathrm{a}}A_1A_3B_1+\Gamma_{10}^{\mathrm{a}}A_3^2B_3+\Gamma_{14}^{\mathrm{a}}A_2A_3B_2)\exp(i\omega_c T_0)+\\&\Gamma_3^{\mathrm{a}}A_1^2B_2\exp(i(2\omega_a-\omega_b)T_0)+\Gamma_5^{\mathrm{a}}A_2^2B_1\exp(i(2\omega_b-\omega_a)T_0)+\\&\Gamma_9^{\mathrm{a}}A_1^2B_3\exp(i(2\omega_a-\omega_c)T_0)+\Gamma_8^{\mathrm{a}}A_3^2B_1\exp(i(2\omega_c-\omega_a)T_0)+\\&\Gamma_{20}^{\mathrm{a}}A_2^2B_3\exp(i(2\omega_b-\omega_c)T_0)-\Gamma_8^{\mathrm{a}}A_3^2B_2\exp(i(2\omega_c-\omega_b)T_0)+\\&\Gamma_7^{\mathrm{a}}B_1A_2A_3\exp(i(\omega_b+\omega_c-\omega_a)T_0)+\Gamma_{17}^{\mathrm{a}}A_1A_3B_2\exp(i(\omega_a-\omega_b+\omega_c)T_0)+\\&\Gamma_{19}^{\mathrm{a}}A_1A_2B_3\exp(i(\omega_a+\omega_b-\omega_c)T_0)+NST_1+cc\end{aligned} \tag{41}$$

$$\begin{aligned}(D_0^2+\omega_b^2)q_{13}=&-i\omega_b(\mu_1A_2+2A_2')\exp(i\omega_b T_0)-ib_{21}\omega_aA_1\exp(i\omega_a T_0)+\\&(\Gamma_2^{\mathrm{b}}A_3+\Gamma_6^{\mathrm{b}}A_1A_3B_1)\exp(i\omega_c T_0)+\Gamma_{14}^{\mathrm{b}}A_3^2B_2\exp(i(2\omega_c-\omega_b)T_0)+\end{aligned}$$

$$(b_{22}\omega_a^2 A_1 + \Gamma_3^b A_1^2 B_1 + \Gamma_{11}^b A_1 A_2 B_2 + \Gamma_{16}^b A_1 A_3 B_3)\exp(i\omega_a T_0) +$$

$$(\Gamma_1^b A_2 + \Gamma_4^b A_1 A_2 B_1 + \Gamma_{12}^b A_2^2 B_2 + \Gamma_{17}^b A_2 A_3 B_3)\exp(i\omega_b T_0) +$$

$$\Gamma_9^b A_1^2 B_2 \exp(i(2\omega_a - \omega_b)T_0) + \Gamma_5^b A_2^2 B_1 \exp(i(2\omega_b - \omega_a)T_0) +$$

$$\Gamma_{10}^b A_1^2 B_3 \exp(i(2\omega_a - \omega_c)T_0) + \Gamma_8^b A_3^2 B_1 \exp(i(2\omega_c - \omega_a)T_0) +$$

$$\Gamma_7^b B_1 A_2 A_3 \exp(i(\omega_b + \omega_c - \omega_a)T_0) + \Gamma_{13}^b A_1 A_3 B_2 \exp(i(\omega_a - \omega_b + \omega_c)T_0) +$$

$$\Gamma_{15}^b A_1 A_2 B_3 \exp(i(\omega_a + \omega_b - \omega_c)T_0) + NST_2 + cc \tag{42}$$

$$(D_0^2 + \omega_c^2)q_{23} = -i\omega_c(\mu_2 A_3 + 2A_3')\exp(i\omega_b T_0) - ib_{31}\omega_a A_1 \exp(i\omega_a T_0) +$$

$$(\Gamma_2^c A_2 + \Gamma_6^c A_1 A_2 B_1)\exp(i\omega_b T_0) + \Gamma_{14}^c A_2^2 B_3 \exp(i(2\omega_b - \omega_c)T_0) +$$

$$(b_{32}\omega_a^2 A_1 + \Gamma_3^c A_1^2 B_1 + \Gamma_{11}^c A_1 A_2 B_2 + \Gamma_{16}^c A_1 A_3 B_3)\exp(i\omega_a T_0) +$$

$$(\Gamma_1^c A_3 + \Gamma_4^c A_1 A_3 B_1 + \Gamma_{12}^c A_3^2 B_3 + \Gamma_{17}^c A_2 A_3 B_3)\exp(i\omega_c T_0) +$$

$$\Gamma_9^c A_1^2 B_3 \exp(i(2\omega_a - \omega_c)T_0) + \Gamma_5^c A_3^2 B_1 \exp(i(2\omega_c - \omega_a)T_0) +$$

$$\Gamma_{10}^c A_1^2 B_2 \exp(i(2\omega_a - \omega_b)T_0) + \Gamma_8^c A_2^2 B_1 \exp(i(2\omega_b - \omega_a)T_0) +$$

$$\Gamma_7^c B_1 A_2 A_3 \exp(i(\omega_b + \omega_c - \omega_a)T_0) + \Gamma_{13}^c A_1 A_2 B_3 \exp(i(\omega_a + \omega_b - \omega_c)T_0) +$$

$$\Gamma_{15}^c A_1 A_3 B_2 \exp(i(\omega_a - \omega_b + \omega_c)T_0) + NST_3 + cc \tag{43}$$

where NST_j (j =1,2,3) denote the non-secular terms and the coefficients Γ_m^n $(n = a,b,c; m = 1,2,3...)$ are defined in Appendix B, respectively. Note that only secular terms except for the external load are retained at right hand of Eqs. (41)-(43).

For the externally primary and subharmonic resonances of this system, $A_j(T_2)$ are expressed in the polar form as follows

$$A_j(T_2) = \frac{1}{2}a_j(T_2)e^{i\psi_j(T_2)}, (\ j = 1,2,3\ ) \tag{44}$$

where a_j and Ψ_j are the amplitude and phase angle of A_j, respectively. In the next section the external primary resonance for the first mode of shallow arch will be disscussed.

4. Primary resonance of the first mode of shallow arch ($\Omega \approx \omega_a$)

4.1 Modulation equations

For exploring external primary resonance of the first mode of shallow arch, we let

$$\Omega = \omega_a + \varepsilon^2 \sigma_1 \tag{45}$$

By substituting Eqs.(44) and (45) into secular terms in Eqs. (41)-(43) and separating the real and imaginary parts, we obtain the modulation equations in the polar form for external primary resonance as follows

$$\begin{aligned}8\omega_a \dot{a}_1 = {} & -4\mu\omega_a a_1 - 4b_{111}\sin\alpha_1 + a_1^2 a_2(\Gamma_4^{\mathrm{a}} - \Gamma_3^{\mathrm{a}})\sin\alpha_2 + a_1 a_2^2 \Gamma_5^{\mathrm{a}} \sin 2\alpha_2 + \Gamma_{12}^{\mathrm{a}} a_2^3 \sin\alpha_2 + \\ & a_1^2 a_3(\Gamma_6^{\mathrm{a}} - \Gamma_9^{\mathrm{a}})\sin\alpha_3 + \left((\Gamma_{19}^{\mathrm{a}} - \Gamma_{17}^{\mathrm{a}})\sin(\alpha_2 - \alpha_3) + \Gamma_7^{\mathrm{a}} \sin(\alpha_2 + \alpha_3)\right) a_1 a_2 a_3 + \\ & a_2^2 a_3 \left(\Gamma_{20}^{\mathrm{a}} \sin(2\alpha_2 - \alpha_3) + \Gamma_{14}^{\mathrm{a}} \sin\alpha_3\right) + a_1 a_3^2 \Gamma_8^{\mathrm{a}} \sin 2\alpha_3 + a_3^3 \Gamma_{10}^{\mathrm{a}} \sin\alpha_3 + \\ & \left((\Gamma_{16}^{\mathrm{a}} \sin\alpha_2 + \Gamma_{13}^{\mathrm{a}} \sin(\alpha_2 - 2\alpha_3)\right) a_2 a_3^2 \end{aligned} \tag{46}$$

$$\begin{aligned}8\omega_a a_1 \dot{\alpha}_1 = {} & 4(\Gamma_1^{\mathrm{a}} + 2\sigma_1\omega_a)a_1 - 4b_{111}\cos\alpha_1 + a_1^2 a_2(\Gamma_4^{\mathrm{a}} + \Gamma_3^{\mathrm{a}})\cos\alpha_2 + a_1 a_2^2(\Gamma_5^{\mathrm{a}} \cos 2\alpha_2 + \Gamma_{11}^{\mathrm{a}}) + \\ & \Gamma_{12}^{\mathrm{a}} a_2^3 \cos\alpha_2 + a_1^2 a_3(\Gamma_6^{\mathrm{a}} + \Gamma_9^{\mathrm{a}})\cos\alpha_3 + a_1 a_2 a_3(\Gamma_{19}^{\mathrm{a}} + \Gamma_{17}^{\mathrm{a}})\cos(\alpha_2 - \alpha_3) + \Gamma_2^{\mathrm{a}} a_1^3 + \\ & a_1 a_2 a_3 \Gamma_7^{\mathrm{a}} \cos(\alpha_2 + \alpha_3) + a_1 a_3^2(\Gamma_{15}^{\mathrm{a}} + \Gamma_{18}^{\mathrm{a}}) + a_2 a_3^2 \left(\Gamma_{16}^{\mathrm{a}} \cos\alpha_2 - \Gamma_{13}^{\mathrm{a}} \cos(\alpha_2 - 2\alpha_3)\right) + \\ & a_2^2 a_3 \left(\Gamma_{20}^{\mathrm{a}} \cos(2\alpha_2 - \alpha_3) + \Gamma_{14}^{\mathrm{a}} \cos\alpha_3\right) + a_1 a_3^2 \Gamma_8^{\mathrm{a}} \cos 2\alpha_3 + a_3^3 \Gamma_{10}^{\mathrm{a}} \cos\alpha_3 \end{aligned} \tag{47}$$

$$\begin{aligned}8\omega_b \dot{a}_2 = {} & -4\mu_1\omega_b a_2 - 4\omega_a(b_{21}\cos\alpha_2 + b_{22}\omega_a \sin\alpha_2)a_1 - \Gamma_3^{\mathrm{b}} a_1^3 \sin\alpha_2 - \Gamma_9^{\mathrm{b}} a_1^2 a_2 \sin 2\alpha_2 + \\ & a_1 a_2^2(\Gamma_5^{\mathrm{b}} - \Gamma_{11}^{\mathrm{b}})\sin\alpha_2 - (4\Gamma_2^{\mathrm{b}} + \Gamma_6^{\mathrm{b}} a_1^2)a_3 \sin(\alpha_2 - \alpha_3) - \Gamma_{10}^{\mathrm{b}} a_1^2 a_3 \sin(\alpha_2 + \alpha_3) - \\ & \Gamma_{16}^{\mathrm{b}} a_1 a_3^2 \sin\alpha_2 - \Gamma_8^{\mathrm{b}} a_1 a_3^2 \sin(\alpha_2 - 2\alpha_3) - (\Gamma_{15}^{\mathrm{b}} - \Gamma_7^{\mathrm{b}})a_1 a_2 a_3 \sin\alpha_3 - \\ & \Gamma_{13}^{\mathrm{b}} a_1 a_2 a_3 \sin(2\alpha_2 - \alpha_3) - \Gamma_{14}^{\mathrm{b}} a_2 a_3^2 \sin(2\alpha_2 - 2\alpha_3) \end{aligned} \tag{48}$$

$$\begin{aligned}8\omega_a\omega_b a_1 a_2 \dot{\alpha}_2 = {} & -\Gamma_3^{\mathrm{b}} \omega_a a_1^4 \cos\alpha_2 - a_1^3 a_2(\Gamma_4^{\mathrm{b}}\omega_a - \Gamma_2^{\mathrm{a}}\omega_b + \Gamma_9^{\mathrm{b}}\omega_a \cos 2\alpha_2) + \Gamma_{12}^{\mathrm{a}} a_2^4 \omega_b \cos\alpha_2 - \\ & a_1^3 a_3 \omega_a \left(\Gamma_6^{\mathrm{b}} \cos(\alpha_2 - \alpha_3) + \Gamma_{10}^{\mathrm{b}} \cos(\alpha_2 + \alpha_3)\right) + \Gamma_{20}^{\mathrm{a}} a_2^2 a_3 \omega_b \cos(2\alpha_2 - \alpha_3) + \\ & a_2^2 a_3 \omega_b \Gamma_{14}^{\mathrm{a}} \cos\alpha_3 + a_2^2 a_3^2 \omega_b \left(\Gamma_{16}^{\mathrm{a}} \cos\alpha_2 - \Gamma_{13}^{\mathrm{a}} \cos(\alpha_2 - 2\alpha_3)\right) + \\ & a_2 a_3^3 \omega_b \Gamma_{10}^{\mathrm{a}} \cos\alpha_3 - a_1^2 a_2^2 \left(\omega_a(\Gamma_{11}^{\mathrm{b}} + \Gamma_5^{\mathrm{b}}) - \omega_b(\Gamma_3^{\mathrm{a}} + \Gamma_4^{\mathrm{a}})\right)\cos\alpha_2 - \\ & a_1^2 a_2 a_3 \left(\left(\omega_a(\Gamma_{15}^{\mathrm{b}} + \Gamma_7^{\mathrm{b}}) - \omega_b(\Gamma_6^{\mathrm{a}} + \Gamma_9^{\mathrm{a}})\right)\cos\alpha_2 + \Gamma_{13}^{\mathrm{b}}\omega_a \cos(2\alpha_2 - \alpha_3)\right) - \\ & 4\omega_a^2 a_1^2(b_{22}\omega_a \cos\alpha_2 - b_{21}\sin\alpha_2) - a_1^2 a_3^2 \omega_a \left(\Gamma_{16}^{\mathrm{b}} \cos\alpha_2 + \Gamma_8^{\mathrm{b}} \cos(\alpha_2 - 2\alpha_3)\right) + \\ & a_1 a_2^3(\Gamma_{11}^{\mathrm{a}}\omega_b - \Gamma_{12}^{\mathrm{b}}\omega_a + \Gamma_5^{\mathrm{a}}\omega_b \cos 2\alpha_2) - 4a_1 a_3 \omega_a \Gamma_2^{\mathrm{b}} \cos(\alpha_2 - \alpha_3) + \end{aligned}$$

$$a_1 a_2^2 \overline{a}_3 \omega_b \left((\Gamma_{17}^{\mathrm{a}} + \Gamma_{19}^{\mathrm{a}}) \cos(\alpha_2 - \alpha_3) + \Gamma_7^{\mathrm{a}} \cos(\alpha_2 + \alpha_3) \right) +$$

$$a_1 a_2 (4\omega_b \Gamma_1^{\mathrm{a}} - 4\omega_a \Gamma_1^{\mathrm{b}} + 8\sigma_2 \omega_a \omega_b - 2b_{12} \omega_b \cos\alpha_1) + a_1 a_2 a_3^2 \omega_b \Gamma_8^{\mathrm{a}} \cos 2\alpha_3 +$$

$$a_1 a_2 a_3^2 \left(\omega_b \Gamma_{15}^{\mathrm{a}} - \Gamma_{17}^{\mathrm{b}} \omega_a - \Gamma_{14}^{\mathrm{b}} \cos(2\alpha_2 - 2\alpha_3) \right) + \omega_b \, a_1 a_2 a_3^2 \Gamma_{18}^{\mathrm{a}} \tag{49}$$

$$8\omega_c \dot{a}_3 = -4\mu_1 \omega_c a_3 - 4\omega_a (b_{31} \cos\alpha_3 + b_{32} \omega_a \sin\alpha_3) a_1 - \Gamma_3^{\mathrm{c}} a_1^3 \sin\alpha_3 - \Gamma_9^{\mathrm{c}} a_1^2 a_3 \sin 2\alpha_3 +$$

$$+ a_1 a_3^2 (\Gamma_5^{\mathrm{c}} - \Gamma_{11}^{\mathrm{c}}) \sin\alpha_3 + (4\Gamma_2^{\mathrm{c}} + \Gamma_6^{\mathrm{c}} a_1^2) \sin(\alpha_2 - \alpha_3) - \Gamma_{10}^{\mathrm{c}} a_1^2 a_2 \sin(\alpha_2 + \alpha_3) -$$

$$a_1 a_2^2 \Gamma_{16}^{\mathrm{c}} \sin\alpha_3 + a_1 a_2^2 \Gamma_8^{\mathrm{c}} \sin(2\alpha_2 - \alpha_3) + (\Gamma_7^{\mathrm{c}} - \Gamma_{15}^{\mathrm{c}}) a_1 a_2 a_3 \sin\alpha_2 +$$

$$\Gamma_{13}^{\mathrm{c}} a_1 a_2 a_3 \sin(\alpha_2 - 2\alpha_3) + \Gamma_{14}^{\mathrm{c}} a_2^2 a_3 \sin(2\alpha_2 - 2\alpha_3) \tag{50}$$

$$8\omega_a \omega_c a_1 a_3 \dot{\alpha}_3 = -\Gamma_3^{\mathrm{c}} \omega_a a_1^4 \cos\alpha_3 - a_1^3 a_3 (\Gamma_4^{\mathrm{c}} \omega_a - \Gamma_2^{\mathrm{a}} \omega_c + \Gamma_9^{\mathrm{c}} \omega_a \cos 2\alpha_3) + \Gamma_{10}^{\mathrm{a}} a_3^4 \omega_c \cos\alpha_3 -$$

$$a_1^3 a_2 \omega_a \left(\Gamma_6^{\mathrm{c}} \cos(\alpha_2 - \alpha_3) + \Gamma_{10}^{\mathrm{c}} \cos(\alpha_2 + \alpha_3) \right) - \Gamma_{13}^{\mathrm{a}} a_2 a_3^3 \omega_c \cos(\alpha_2 - 2\alpha_3)$$

$$+ a_2^3 a_3 \omega_c \Gamma_{12}^{a} \cos\alpha_2 + a_2^2 a_3^2 \omega_c \left(\Gamma_{14}^{\mathrm{a}} \cos\alpha_3 + \Gamma_{20}^{\mathrm{a}} \cos(2\alpha_2 - \alpha_3) \right)$$

$$+ a_2 a_3^3 \omega_c \Gamma_{16}^{\mathrm{a}} \cos\alpha_2 - a_1^2 a_3^2 \left(\omega_a (\Gamma_{11}^{\mathrm{c}} + \Gamma_5^{\mathrm{c}}) - \omega_c (\Gamma_6^{\mathrm{a}} + \Gamma_9^{\mathrm{a}}) \right) \cos\alpha_3$$

$$- a_1^2 a_2 a_3 \left(\left(\omega_a (\Gamma_{15}^{\mathrm{c}} + \Gamma_7^{\mathrm{c}}) - \omega_c (\Gamma_3^{\mathrm{a}} + \Gamma_4^{\mathrm{a}}) \right) \cos\alpha_2 + \Gamma_{13}^{\mathrm{c}} \omega_a \cos(\alpha_2 - 2\alpha_3) \right)$$

$$- 4\omega_a^2 a_1^2 (b_{32} \omega_a \cos\alpha_3 - b_{31} \sin\alpha_3) - a_1^2 a_2^2 \omega_a \left(\Gamma_{16}^{\mathrm{c}} \cos\alpha_3 + \Gamma_8^{\mathrm{c}} \cos(2\alpha_2 - \alpha_3) \right)$$

$$+ a_1 a_3^3 \left(\Gamma_{15}^{\mathrm{a}} \omega_c - \Gamma_{12}^{\mathrm{c}} \omega_a + \Gamma_8^{\mathrm{a}} \omega_c \cos 2\alpha_3 \right) - 4a_1 a_2 \omega_a \Gamma_2^{\mathrm{c}} \cos(\alpha_2 - \alpha_3)$$

$$+ a_1 a_2 a_3^2 \omega_c \left((\Gamma_{17}^{\mathrm{a}} + \Gamma_{19}^{\mathrm{a}}) \cos(\alpha_2 - \alpha_3) + \Gamma_7^{\mathrm{a}} \cos(\alpha_2 + \alpha_3) \right)$$

$$+ a_1 a_3 (4\omega_c \Gamma_1^{\mathrm{a}} - 4\omega_a \Gamma_1^{\mathrm{c}} + 8\sigma_3 \omega_a \omega_c - 2b_{12} \omega_c \cos\alpha_1) + a_1 a_2^2 a_3 \omega_c \Gamma_5^{\mathrm{a}} \cos 2\alpha_2$$

$$- a_1 a_2^2 a_3 \left(\Gamma_{11}^{\mathrm{a}} \omega_c - \Gamma_{17}^{\mathrm{c}} \omega_a - \Gamma_{14}^{\mathrm{c}} \omega_a \cos(2\alpha_2 - 2\alpha_3) \right) + \omega_c a_1 a_3^3 \Gamma_{18}^{\mathrm{a}} \tag{51}$$

where

$$\alpha_1(T_2) = \sigma T_2 - \psi_1(T_2)$$

$$\alpha_2(T_2) = \sigma_1 T_2 - \psi_1(T_2) + \psi_2(T_2)$$

$$\alpha_3(T_2) = \sigma_2 T_2 - \psi_1(T_2) + \psi_3(T_2)$$

The stable equilibrium solutions of the modulation Eqs. (46)-(51) corresponding to steady periodic motion of cables and shallow arch, which can be determined by setting $\dot{a}_j = \dot{\alpha}_j = 0$ ($j = 1, 2, 3$)

in the modulation equations and solving the nonlinear system by using the Newton-Rahson method. In order to determine the stability of these equilibrium solutions, one need to evaluate the eigenvalues of Jacobian matrix of the dynamic system and check whether the real part of each eigenvalue is negative or not. In the following, the stable and unstable solutions are indicated, respectively, by thick and thin lines. From Eqs. (46)-(51), it is noted that the complex mode interaction is possible for these modulation equations, which will be discussed in next section. The SN and HB are used to denote the saddle-node bifurcations and Hopf bifurcations, respectively.

4.2 Parameters of cables and shallow arch

In order to explore the nonlinear dynamic behaviors of the double-cable-stayed shallow-arch system subjected to external primary or subharmonic resonance by using the these modulation equations as shown in Eqs (46)-(51) or (48),(50) and (53)-(56), we choose the following parameters and material properties of shallow arch and cables. For shallow arch(Zhou and Chen,2016): Young's modulus E_{a} =2.0$\times 10^{11}$ Pa, length L =300 m, moment of inertia I_{a} =1.2 m^4, area A_{a} =2.15 m^2 and density ρ_{a} =7.8498$\times 10^3$kg/m^3. It is notable that the natural frequency of shallow arch is subtle to the initial shallow arch axis illustrated by y_{a} , where, $y_{\mathrm{a}} = (h_a / 2)(1-\cos 2\pi s)$ (Yi et al., 2014). h_a denotes the non-dimensional rise of shallow arch and is less than or equal to 0.05. h_a is used to adjust easily the frequency of global mode as shown in Fig. 4. Obviously, the non-dimensional rise varies in different cable-stayed bridges, which leads to different global mode frequency. Simultaneously, there are many cables with different properties, which lead to the match of frequencies of local modes of cables and global modes of bridge. Hence, complex modal interaction may exist for this kind of bridge. For cables, Young's modulus E_{l} =2.1$\times 10^{11}$ Pa, length L_{l} =200 m, area A_{l}=7.8$\times 10^{-3}$ m^2 and the density ρ_{l} =6.233$\times 10^3$kg/m^3. The initial equilibrum configurations y_j (j=1,2) for inclined cables are described through the parabola $y_j = 4d_j(x_j/l_j - (x_j/l_j)^2)$ under the assumptions of small sag d_j to length l_j (Gattulli et al.,2002). For exploring the one-to-one-to-one internal resonance between cables and shallow arch, the second cable has the identical properties with the first one. These parameters of cables and shallow arch give the values of non-dimensional quantities in Eq. (10) as shown in Table 1. Furthermore, we choose the sine function as the mode shapes of cables and shallow arch, namely, $\phi(s) = \sin \pi s$ and $\varphi_i(x_i) = \sin \pi x_i$ (Kang et al., 2013). The relatively low excitation amplitudes (B=0.0001-0.0004) and small damping coefficients (μ_i=0.003,i=1,2,3) are also used in the following numerical calculation.

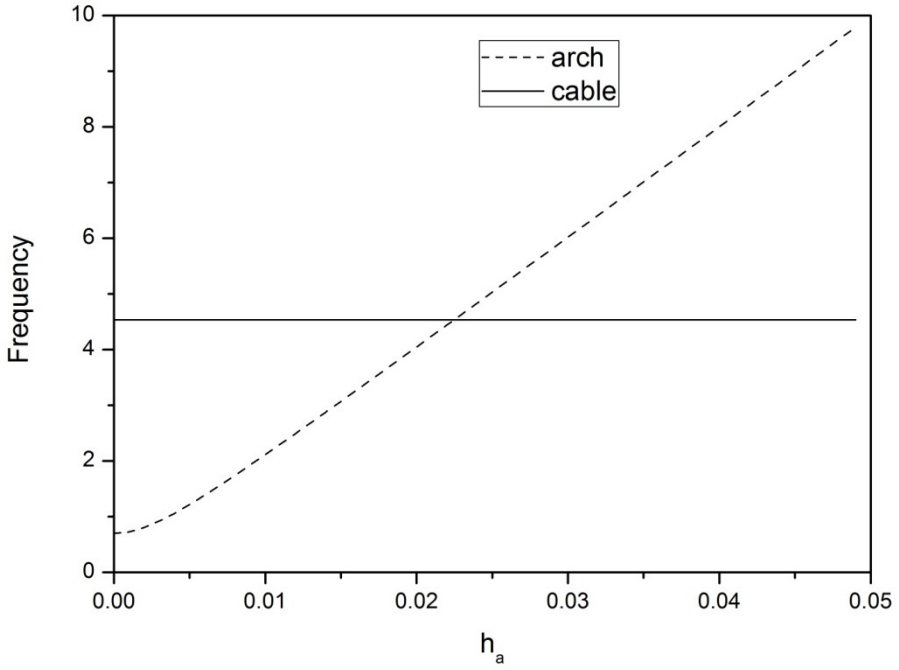

Fig.4 Variation of non-dimensional frequency with non-dimensional rise of shallow arch

Table 1. Frequencies and Non-dimensional parameters of cables and shallow arch

cable				shallow arch		
$\omega_b(\omega_c)$	$K_1(K_2)$	$\lambda_1(\lambda_2)$	$\beta_1(\beta_2)$	ω_a	β	η
4.53763	1.61157	409.5	0.69728	4.63763	4.88986	161850

Note: ω_a , ω_b and ω_c are the circular frequency.

4.3 Numerical calculation and discussion

As we have seen, the derivation of these modulation equations is relatively complex. In order to verify the accuracy of the following results obtained by the pseudo arclength algorithm (Seydel,2009) based on the proposed theories, the fourth-order Runge-Kutta method are used to integrate directly these Eqs. (21)-(23) until the steady motion of the system are arrived (Parker and Chua,1989), which are denoted by star and can be seen in Fig.5. It should be noted that the jumping phenomena can be captured by both upward and downward scanning of σ_1 and the results of previous step are regarded as the initial conditions of the next step in calculation by the fourth-order Runge-Kutta method. As seen, the agreement is satisfactory. Hence, the other results are obtained by the pseudo arclength algorithm due to its convenience and accuracy. The frequency responses diagrams (see Figs. 3, 4 and 7) and amplitude responses figures (see Figs.5 and 6) are constructed to explore the dynamic behaviors of the double-cable-stayed shallow-arch system.

There are two peaks in Fig. 5(b) for cables, one bent to the left and one bent to the right. This is associated with a double jumping phenomenon (Chen et al.,2014; Guo et al., 2016) in the frequency response diagrams, which is triggered by those saddle-node bifurcations, i.e., SN1, SN2. Actually, it can be deduced that there exists two saddle-node bifurcations at the left and right side beyond the range [-1.5,1.5] of σ_1, respectively. For $\sigma_1<0$, the cables exhibit soft-spring while for $\sigma_1>0$ they behave hard-spring. When $\sigma_1>0$, with increasing of σ_1 the equilibrium solutions of cables and arch turn unstable through a Hopf bifurcation at HB1, and regain stability at HB2. In the small range of σ_1 between the two Hopf bifurcations, there exist stable and unstable periodic solutions and the response amplitudes a_2 and a_3 of cables are relatively big. Hence, the Hopf bifurcations should be controlled in engineering. All these phenomena for cables are similar to those got by Guo et. al (Guo et al., 2016) due to the fact that the motion of cables are excited at the lower ends of cables. However, there exist

apparently differences between them. The symmetry of the frequency response diagrams of cable does not exist due to the impact of coupled motion with shallow arch. It can be seen from Fig. 5(a) that the shallow arch always behaves soft-spring property in the whole range of σ_1 and the two stable branches exist closely as σ_1>0.686.

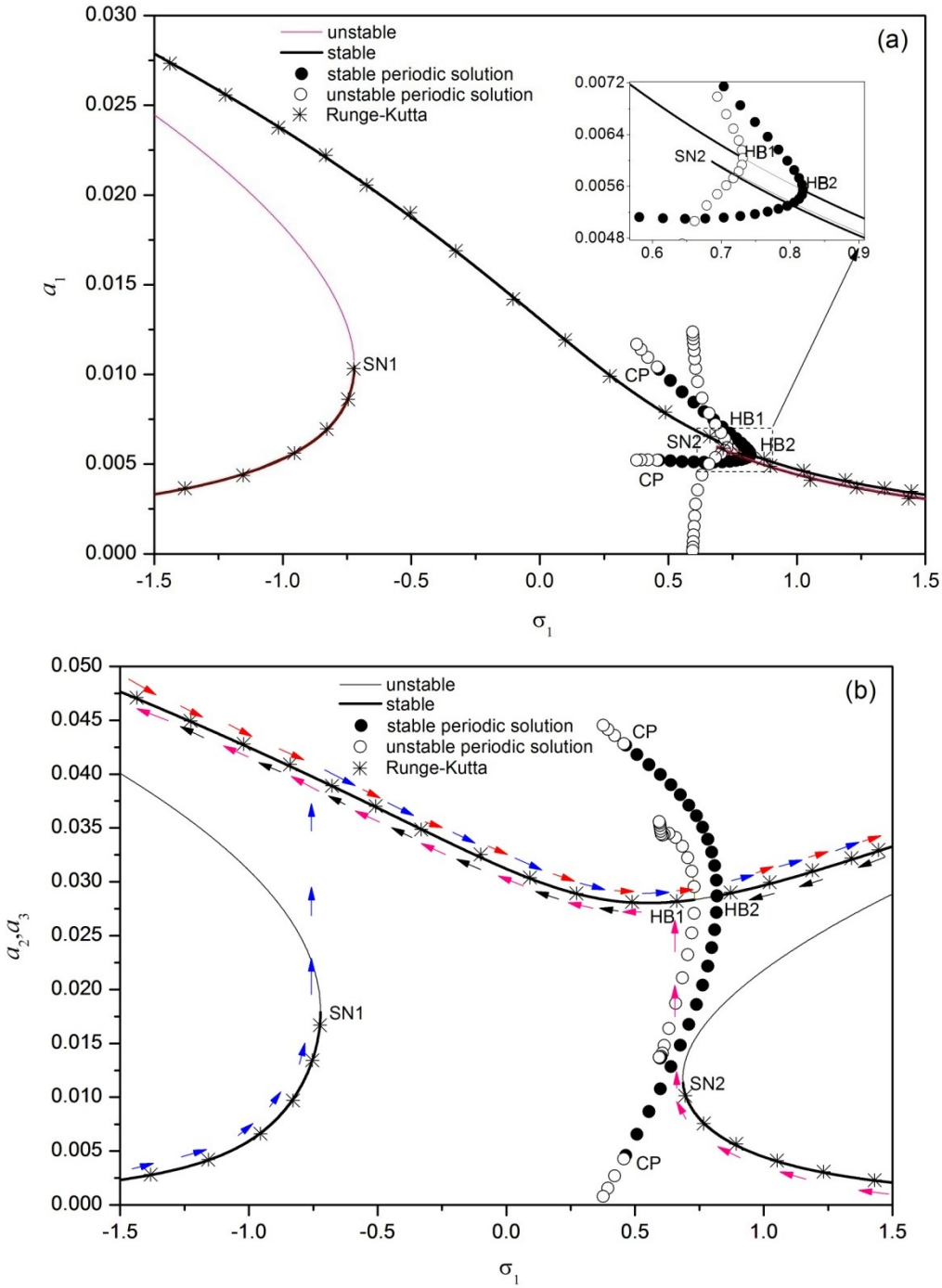

Fig. 5 Frequency response curves of modal amplitudes a_1, a_2 and a_3 to excitation amplitude B=0.0004 with $\sigma_2=\sigma_3=-0.1$: (a) for shallow arch and (b) for cables.

Additionally, an interesting phenomenon is observed for the two identical cables. As seen in Fig. 5(b), there exists two stable branches as σ_1<-0.72 or σ_1>0.686. For the two identical cables, sometimes they behave simultaneously identical motion namely, the equilibrium solutions are the upper branch or the lower branch even that the different initial conditions are given. Sometimes, they behave different motions even the identical initial conditions are given. This means that the two identical cables sometimes have different equilibrium solutions, namely, the upper branch is for one cable and the lower branch for the other. Here, it should be illustrated that the two cables are located at shallow arch

symmetrically shown in Fig.3. In other words, the two different stable equilibrium solutions of cable can be exhibited simultaneously by two identical cables. This novel phenomenon can be used explain why the vibration of cable can be observed in some cables or cable-stayed bridge.

Fig.6 presents the frequency response curves of modal amplitudes a_1, a_2 and a_3 to different excitation amplitudes. It is observed that the responses not only for cables but for shallow arch increase with the increasing of the excitation amplitude with the same excitation frequency. It is also noted that the frequency range between the two saddle-node bifurcations for large vibration of cables and arch expands with the increasing of the excitation amplitude.

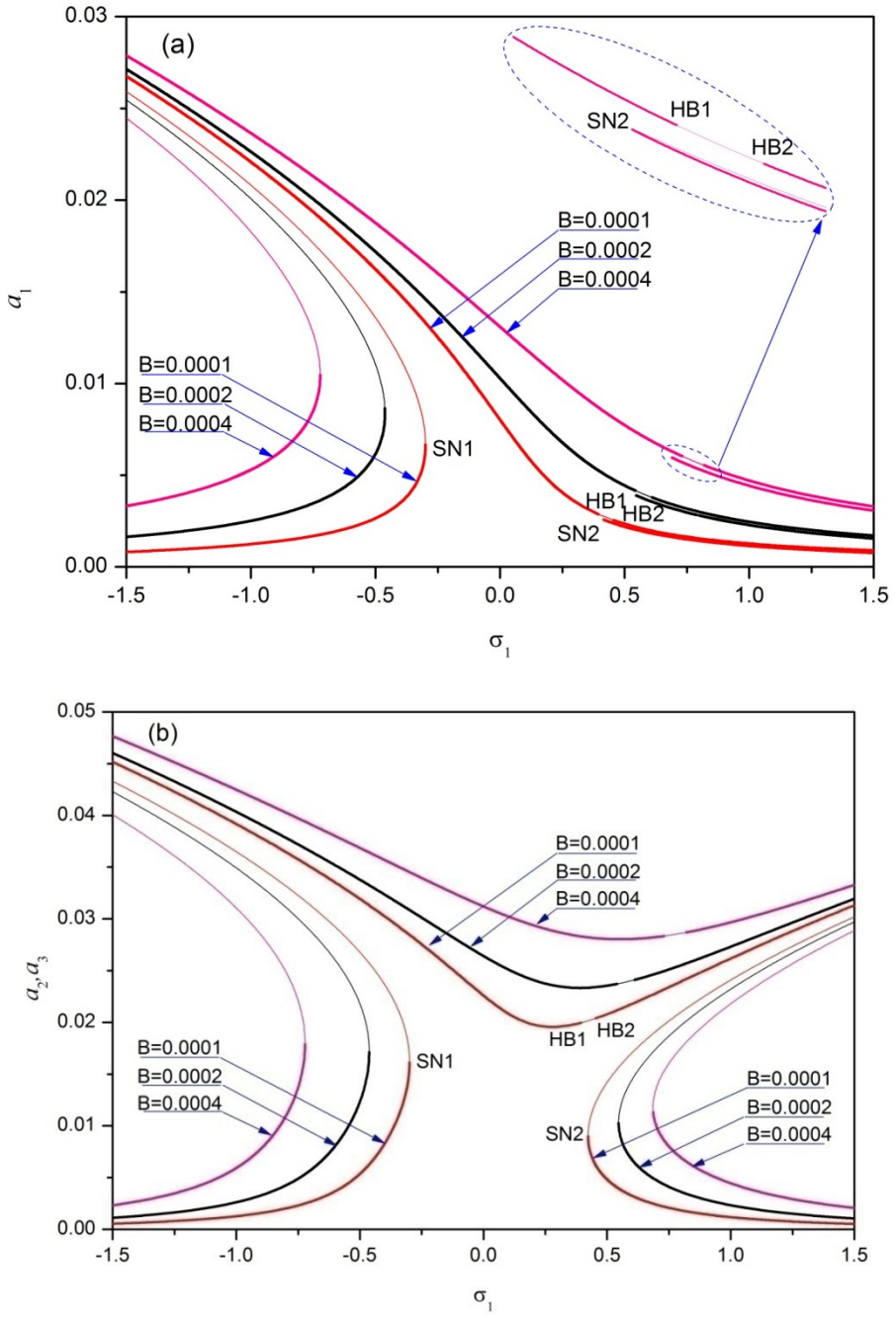

Fig. 6 Frequency response curves of modal amplitudes a_1, a_2 and a_3 to different excitation amplitudes with σ_2=σ_3=-0.1: (a) for shallow arch and (b) for cables.

Furthermore, the frequency range for periodic motion between the two Hopf bifurcations is also enlarged. The response of shallow arch is small as σ_1>0, but the response of two cable may be very big as shown in Figs. 5 and 6. This means that the vibration control of deck may be useless for reducing

large motion of cables in cable-stayed bridge. Similarly, reducing the axial excitation amplitude at the right end of shallow arch may be also fruitless because that the stable equilibrium solutions (the upper branch) is not susceptive to the excitation amplitude, although the response amplitude decreases to a certain extent.

By sweeping the excitation amplitude B (i.e., the right end support motion of the shallow arch) , the amplitude-response diagrams are also constructed similarly (with σ_1= 0.5 shown in Fig. 7 and σ_1= 0, -0.5 shown in Fig.8).

For $\sigma_1 = -0.5 < 0$, as illustrated in Fig. 8, the jumping phenomenon also exists and is triggered by saddle-node bifurcations SN1 and SN2. It is noted that when the excitation amplitude B decreases the upper stable branch jumps to zero at SN2 through the saddle-node bifurcation. Furthermore, the saddle-node bifurcation (with $\sigma_1 = 0$) disappears as shown in Fig.8. However, for $\sigma_1 = 0.5 > 0$, the dynamic behavior of the system becomes complex as shown in Fig. 7.

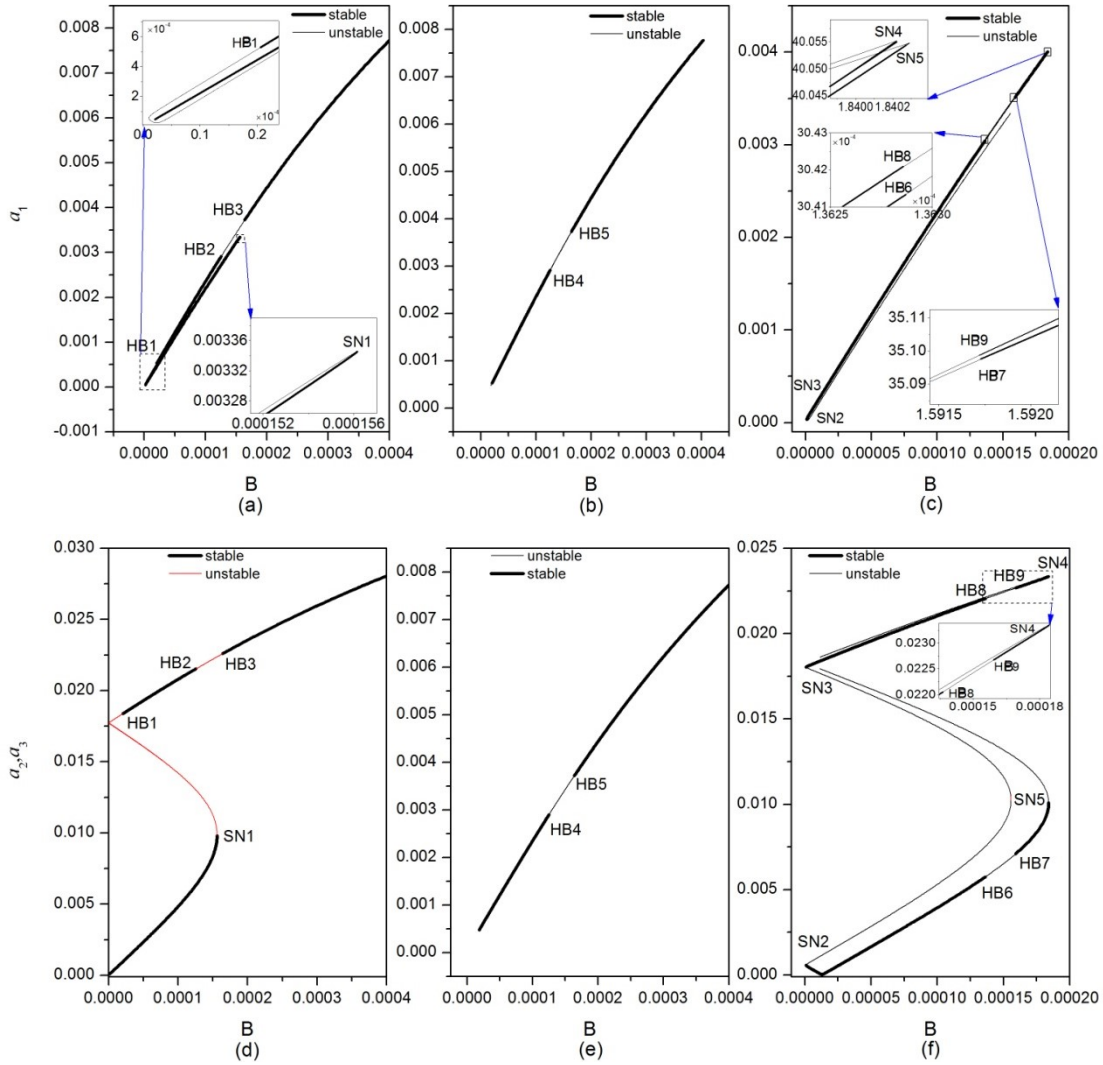

Fig.7 Modal amplitudes a_1, a_2 and a_3 for increasing excitation amplitude with σ_1=0.5 and σ_2=σ_3=-0.1: (a)-(c) for shallow arch and (e)-(f) for cables.

With the excitation amplitude B increasing from zero, as shown in Figs. 5(a) and (d), the coupled stable responses of cables and shallow arch increase sharply, then jump to the upper branch by the saddle-node bifurcation (SN1) and lose their stable simultaneously, and then regain the stable through the Hopf bifurcation (HB3) with the further increasing of excitation amplitude B. Reversely, with the

excitation amplitude decreasing from 0.0004, the responses decrease and lose their stable at HB3, then regain their stable at HB2, and lose their stable at HB1 and jump to the lower branch. It is interesting that the jumping phenomenon may not occur if the equilibrium solutions go alone the other branch as shown in Figs. 5(b) and (e) while the Hopf bifurcations also exist. At the same time, the responses of cables become relatively small. It needs to be noted that the two cables may behave different dynamic properties due to the multi-branch of solutions.

When the excitation amplitude is less than 0.0002 as shown in Figs. 5(c) and (f), with its decreasing the upper stable solutions lose their stable at HB9 and regain the stable at HB8, and then jump to the lower stable branch through saddle-node bifurcation (SN3 and SN2). If the excitation amplitude is increased from zero, the lower stable solutions will lose and regain their stable through Hopf bifurcations at HB6 and HB7, respectively, and then jump to the upper stable branch through the saddle-node bifurcations, i.e., SN5 and SN4.

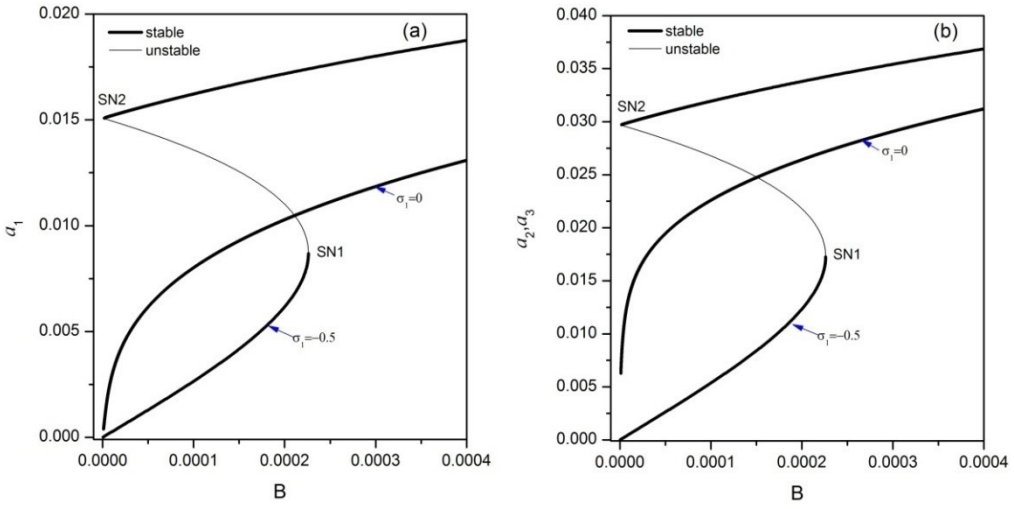

Fig.8 Modal amplitudes a_1, a_2 and a_3 for increasing excitation amplitude with σ_2=σ_3=-0.1: (a) for shallow arch and (b) for cables.

In order to explore the influence of different cables on the dynamics of double-cable-stayed shallow arch system, one of the cable is same as the aforementioned parameter (here named cable 1#) and the other (cable 2#) is changed by σ_3 , which can indicate the variation of the length, initial force, the cross-section area, incline angle and Young's modulus of cable. The variation of Young's modulus of cable can be used to model the new CFRP cable, where CFRP is short of Carbon Fibre Reinforced Plastic. Fig.9 illustrates the frequency-response curves of modal amplitudes a_1, a_2 and a_3 with excitation amplitude B=0.0004. It needs to be explained that the two modulation parameters σ_2 and σ_3 are changed with the variation of the second cable's parameters because that the frequency of global mode is also changed. It is obviously that the parameter variation of cable 2# can influence the local dynamics of other cable and the global dynamics of shallow arch. In the following, the new dynamic phenomenon is our focus and the similar properties as aforementioned in Fig. 5 have been ignored.

As seen in Fig. 9.1, with the increasing of σ_1 from -1.5, the unstable and stable equilibrium solutions shift alternately through those Hopf bifurcations, i.e., HB1,HB2,HB3,HB4,HB5. Obviously, the dynamic behaviors of cables and shallow arch become more complex than those of two identical cables. A new stable equilibrium solution appears as σ_1>0.686, which means that

there exist three stable equilibrium solutions in a certain interval. Additionally, for cable 1#, the saddle-node bifurcation occurs in the middle stable branch while it appears in the lower stable branch for cable 2#.

With the difference between the two cables increasing, namely, σ_2=0.78 and σ_3=-0.8, as shown in Fig. 9.2, the lower stable equilibrium branch vanishes for cable 1# when σ_1>0. It is noted that for cable 2# the response amplitude a_3 increases, nearly up to 20% while there is almost no changes for cable 1#.

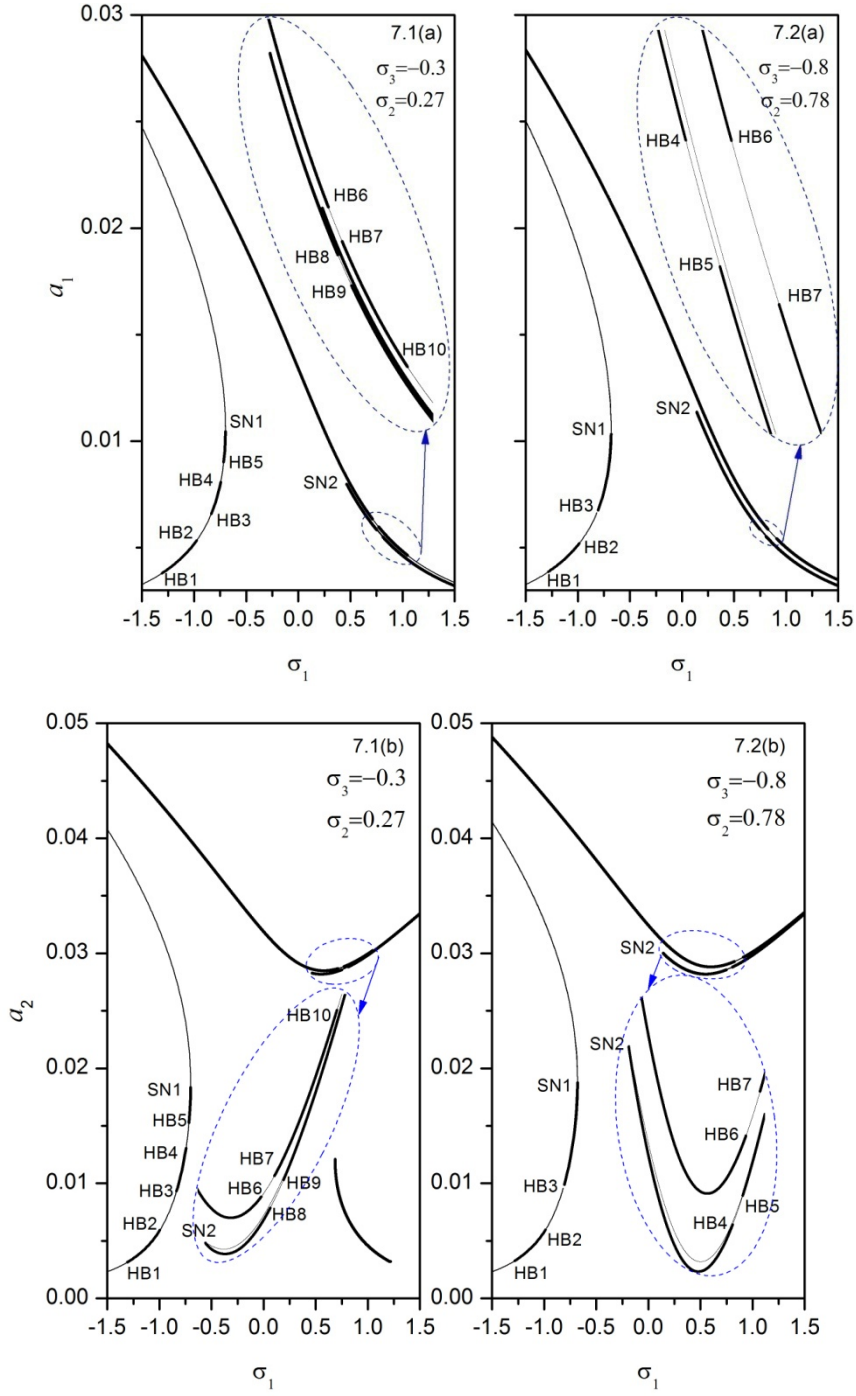

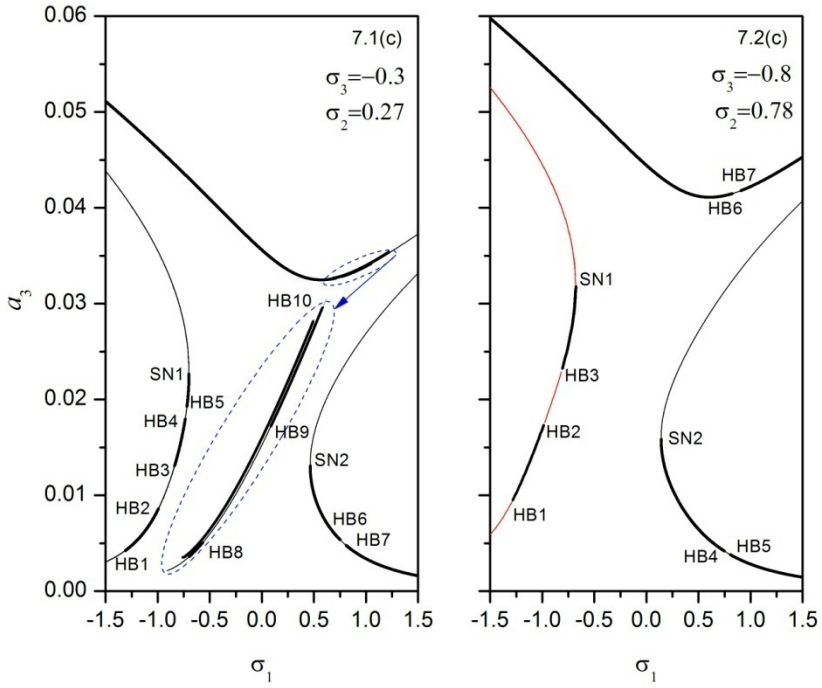

Fig. 9 Frequency response curves of modal amplitudes a_1, a_2 and a_3 to excitation amplitude B=0.0004 with σ_2=-0.1: (a) for shallow arch and (b) for cables.

5. Subharmonic resonance of the first mode of shallow arch ($\Omega \approx 2\omega_a$)

5.1 Modulation equations

For the external subharmonic resonance of the first mode of shallow arch, we let

$$\Omega = 2\omega_a + \varepsilon^2\sigma_1 \tag{52}$$

Similarly, we obtain the modulation equations in the polar form for external subharmonic resonance as follows

$$\begin{aligned}8\omega_a\dot{a}_1 = {} & -4\mu\omega_a a_1 - 2b_{12}a_1\sin\alpha_1 + a_1^2a_2(\Gamma_4^{\mathrm{a}} - \Gamma_3^{\mathrm{a}})\sin\alpha_2 + a_1a_2^2\Gamma_5^{\mathrm{a}}\sin 2\alpha_2 + \Gamma_{12}^{\mathrm{a}}a_2^3\sin\alpha_2 + \\ & a_1^2a_3(\Gamma_6^{\mathrm{a}} - \Gamma_9^{\mathrm{a}})\sin\alpha_3 + \left((\Gamma_{19}^{\mathrm{a}} - \Gamma_{17}^{\mathrm{a}})\sin(\alpha_2 - \alpha_3) + \Gamma_7^{\mathrm{a}}\sin(\alpha_2 + \alpha_3)\right)a_1a_2a_3 + \\ & a_2^2a_3\left(\Gamma_{20}^{\mathrm{a}}\sin(2\alpha_2 - \alpha_3) + \Gamma_{14}^{\mathrm{a}}\sin\alpha_3\right) + a_1a_3^2\Gamma_8^{\mathrm{a}}\sin 2\alpha_3 + a_3^3\Gamma_{10}^{\mathrm{a}}\sin\alpha_3 + \\ & \left((\Gamma_{16}^{\mathrm{a}}\sin\alpha_2 + \Gamma_{13}^{\mathrm{a}}\sin(\alpha_2 - 2\alpha_3)\right)a_2a_3^2\end{aligned} \tag{53}$$

$$\begin{aligned}4\omega_a a_1\dot{\alpha}_1 = {} & 4(\Gamma_1^{\mathrm{a}} + \sigma_1\omega_a)a_1 - 2b_{12}a_1\cos\alpha_1 + a_1^2a_2(\Gamma_4^{\mathrm{a}} + \Gamma_3^{\mathrm{a}})\cos\alpha_2 + a_1a_2^2(\Gamma_5^{\mathrm{a}}\cos 2\alpha_2 + \Gamma_{11}^{\mathrm{a}}) + \\ & \Gamma_{12}^{\mathrm{a}}a_2^3\cos\alpha_2 + a_1^2a_3(\Gamma_6^{\mathrm{a}} + \Gamma_9^{\mathrm{a}})\cos\alpha_3 + a_1a_2a_3(\Gamma_{19}^{\mathrm{a}} + \Gamma_{17}^{\mathrm{a}})\cos(\alpha_2 - \alpha_3) + \Gamma_2^{\mathrm{a}}a_1^3 + \\ & a_1a_2a_3\Gamma_7^{\mathrm{a}}\cos(\alpha_2 + \alpha_3) + a_1a_3^2(\Gamma_{15}^{\mathrm{a}} + \Gamma_{18}^{\mathrm{a}}) + a_2a_3^2\left(\Gamma_{16}^{\mathrm{a}}\cos\alpha_2 - \Gamma_{13}^{\mathrm{a}}\cos(\alpha_2 - 2\alpha_3)\right) + \\ & a_2^2a_3\left(\Gamma_{20}^{\mathrm{a}}\cos(2\alpha_2 - \alpha_3) + \Gamma_{14}^{\mathrm{a}}\cos\alpha_3\right) + a_1a_3^2\Gamma_8^{\mathrm{a}}\cos 2\alpha_3 + a_3^3\Gamma_{10}^{\mathrm{a}}\cos\alpha_3\end{aligned} \tag{54}$$

$$8\omega_a\omega_b a_1 a_2\dot{\alpha}_2 = 4b_{21}\omega_a^2 a_1^2\sin\alpha_2 - 4a_1a_2(\Gamma_1^{\mathrm{b}}\omega_a - \Gamma_1^{\mathrm{a}}\omega_b) + 2\omega_b a_1 a_2(4\sigma_1\omega_a - a_2\cos\alpha_1) -$$

$$a_1^3 a_2\left(\Gamma_4^{\mathrm{b}}\omega_a + \Gamma_2^{a}\omega_b\right) - a_2^3 a_1\left(\Gamma_{12}^{\mathrm{b}}\omega_a - \Gamma_{11}^{a}\omega_b\right) - a_1a_2\left(\Gamma_9^{\mathrm{b}}\omega_a a_1^2 - \Gamma_5^{a}\omega_b a_2^2\right)\cos(2\alpha_2) -$$

$$\left(\Gamma_{13}^{\mathrm{b}}a_1^2\omega_a + \Gamma_{20}^{\mathrm{a}}a_2^2\omega_b\right)a_2a_3\cos(2\alpha_2 - \alpha_3) - a_2a_3a_3^2\left(\Gamma_{17}^{\mathrm{b}}\omega_a + \Gamma_{15}^{\mathrm{a}}\omega_b\right) +$$

$$a_1 a_2 a_3^2\omega_b\left(\Gamma_{18}^{\mathrm{a}} + \Gamma_8^{\mathrm{a}}\cos(2\alpha_3)\right) - \Gamma_{14}^{\mathrm{b}}a_1 a_2 a_3^2\omega_a\cos\left(2\alpha_2 - 2\alpha_3\right) +$$

$$a_1a_3\left((\Gamma_{17}^{\mathrm{a}} + \Gamma_{19}^{\mathrm{a}})\omega_b a_2^2 - \omega_a(4\Gamma_2^{\mathrm{b}} + \Gamma_6^{\mathrm{b}}a_1^2)\right)\cos(\alpha_2 - \alpha_3) +$$

$$a_1a_3(\Gamma_7^{\mathrm{a}}a_2^2\omega_b - \Gamma_{10}^{\mathrm{b}}a_1^2\omega_a)\cos(\alpha_2 + \alpha_3) - a_3^2\left(\Gamma_{13}^{a}\omega_b a_2^2 + \Gamma_8^{\mathrm{b}}\omega_a a_1^2\right)\cos(\alpha_2 - 2\alpha_3) -$$

$$\left(a_1^2\omega_a(4b_{22}\omega_a^2 + \Gamma_3^{\mathrm{b}}a_1^2) + \overline{a}_2^2(\Gamma_{11}^{\mathrm{b}}a_1^2\omega_a - \Gamma_{12}^{\mathrm{a}}a_2^2\omega_b)\right)\cos\alpha_2 -$$

$$\left(a_1^2a_2^2(\Gamma_5^{\mathrm{b}}\omega_a - \Gamma_3^{\mathrm{a}}\omega_b - \Gamma_4^{a}\omega_b) + a_3^2(\Gamma_{16}^{\mathrm{b}}a_1^2\omega_a - \Gamma_{16}^{\mathrm{a}}a_2^2\omega_b)\right)\cos\alpha_2 +$$

$$+ a_2a_3\left(\omega_b(\Gamma_{14}^{\mathrm{a}}a_2^2 + \Gamma_{10}^{\mathrm{a}}a_3^2) - (\Gamma_{15}^{\mathrm{b}}\omega_a + \Gamma_7^{\mathrm{b}}\omega_a - \Gamma_6^{\mathrm{a}}\omega_b - \Gamma_9^{\mathrm{a}}\omega_b)a_1^2\right)\cos\alpha_3 \qquad (55)$$

$$8\omega_a\omega_c a_1 a_3\dot{\alpha}_3 = \omega_a a_1^2\left(4b_{31}\omega_a\sin\alpha_3 - \Gamma_5^{\mathrm{c}}a_2^2\cos(2\alpha_2 - \alpha_3)\right) + \Gamma_{20}^{\mathrm{a}}a_2^2a_3^2\omega_c\cos(2\alpha_2 - \alpha_3) -$$

$$2a_1a_3\left(2\Gamma_2^{\mathrm{c}}\omega_a - 2\Gamma_1^{a}\omega_c - 4\sigma_2\omega_a\omega_c + b_{12}\omega_c\cos\alpha_1\right) -$$

$$a_1^3a_3\left(\Gamma_6^{\mathrm{c}}\omega_a - \Gamma_2^{\mathrm{a}}\omega_c + \Gamma_{10}^{\mathrm{c}}\omega_a\cos(2\alpha_2)\right) - a_1a_3a_2^2\Gamma_{15}^{\mathrm{c}}\omega_a\cos(2\alpha_2 - 2\alpha_3) -$$

$$a_1a_3a_2^2\left(\Gamma_{17}^{\mathrm{c}}\omega_a - \Gamma_{11}^{\mathrm{a}}\omega_c + \Gamma_5^{\mathrm{a}}\omega_c\cos(2\alpha_2)\right) + a_1a_3^3\omega_c(\Gamma_{15}^{\mathrm{a}} + \Gamma_{18}^{\mathrm{a}}) -$$

$$a_1a_3^3\left(\Gamma_{13}^{\mathrm{c}}\omega_a + \Gamma_8^{\mathrm{a}}\omega_c\cos(2\alpha_2)\right) + a_1a_2a_3^2\omega_c(\Gamma_{17}^{\mathrm{a}} + \Gamma_{19}^{\mathrm{a}})\cos(\alpha_2 - \alpha_3) -$$

$$a_1a_2\omega_a(4\Gamma_1^{\mathrm{c}} + \Gamma_4^{\mathrm{c}}a_1^2)\cos(\alpha_2 - \alpha_3) - a_1a_2\left(\Gamma_9^{\mathrm{c}}\omega_a a_1^2 - \Gamma_7^{\mathrm{a}}\omega_c a_3^2\right)\cos(\alpha_2 + \alpha_3) -$$

$$a_2a_3\left(\Gamma_{14}^{\mathrm{c}}\omega_a a_1^2 + \Gamma_{13}^{\mathrm{a}}\omega_c a_3^2\right)\cos(\alpha_2 - 2\alpha_3) + a_2a_3\omega_c\left(\Gamma_{12}^{\mathrm{a}}a_2^2 + \Gamma_{16}^{\mathrm{a}}a_3^2\right)\cos\alpha_2 -$$

$$a_1^2a_2a_3\left(\Gamma_7^{\mathrm{c}}\omega_a - \Gamma_{12}^{\mathrm{c}}\omega_a - \Gamma_3^{\mathrm{a}}\omega_c - \Gamma_4^{\mathrm{a}}\omega_c\right)\cos\alpha_2 + \omega_c\,\Gamma_{10}^{\mathrm{a}}a_3^4\cos\alpha_3 +$$

$$\omega_c a_3^2\left(\Gamma_9^{\mathrm{a}}a_1^2 + \Gamma_{14}^{\mathrm{a}}a_2^2\right)\cos\alpha_3 - \omega_a a_1^2\left(4b_{32}\omega_a^2 + \Gamma_3^{\mathrm{c}}a_1^2 + \Gamma_{11}^{\mathrm{c}}a_2^2\right)\cos\alpha_3 -$$

$$a_1^2a_3^2\left(\Gamma_{16}^{\mathrm{c}}\omega_a + \Gamma_8^{\mathrm{c}}\omega_a - \Gamma_6^{\mathrm{a}}\omega_c\right)\cos\alpha_3 \qquad (56)$$

where the others modulation equations for two cables are identical with Eqs. (48) and (50), and $\alpha_1(T_2) = \sigma_1 T_2 - 2\psi_1(T_2)$.

5.2 Numerical calculation

Fig. 10 shows the frequency–response curves for the first modes of cables and shallow arch when the first mode of the latter is excited by a subharmonic resonance for σ2=-0.14 and

σ3=-0.14. As can be noted from the figure, although multiple stable and unstable solutions exist for the three modes of cables and shallow arch, the dynamic behavior is simpler than that of the system under primary resonance. Saddle-node bifurcations are observed, however the jump phenomenon are not identified. Furthermore, Hopf bifurcations occur only if the excitation amplitude is greater than a threshold value. Additionally, it is noted that the response of shallow arch trends to zero but those of cables increase for $\sigma_1>0$, which is similar to those discussed earlier as shown in Fig. 6(b).

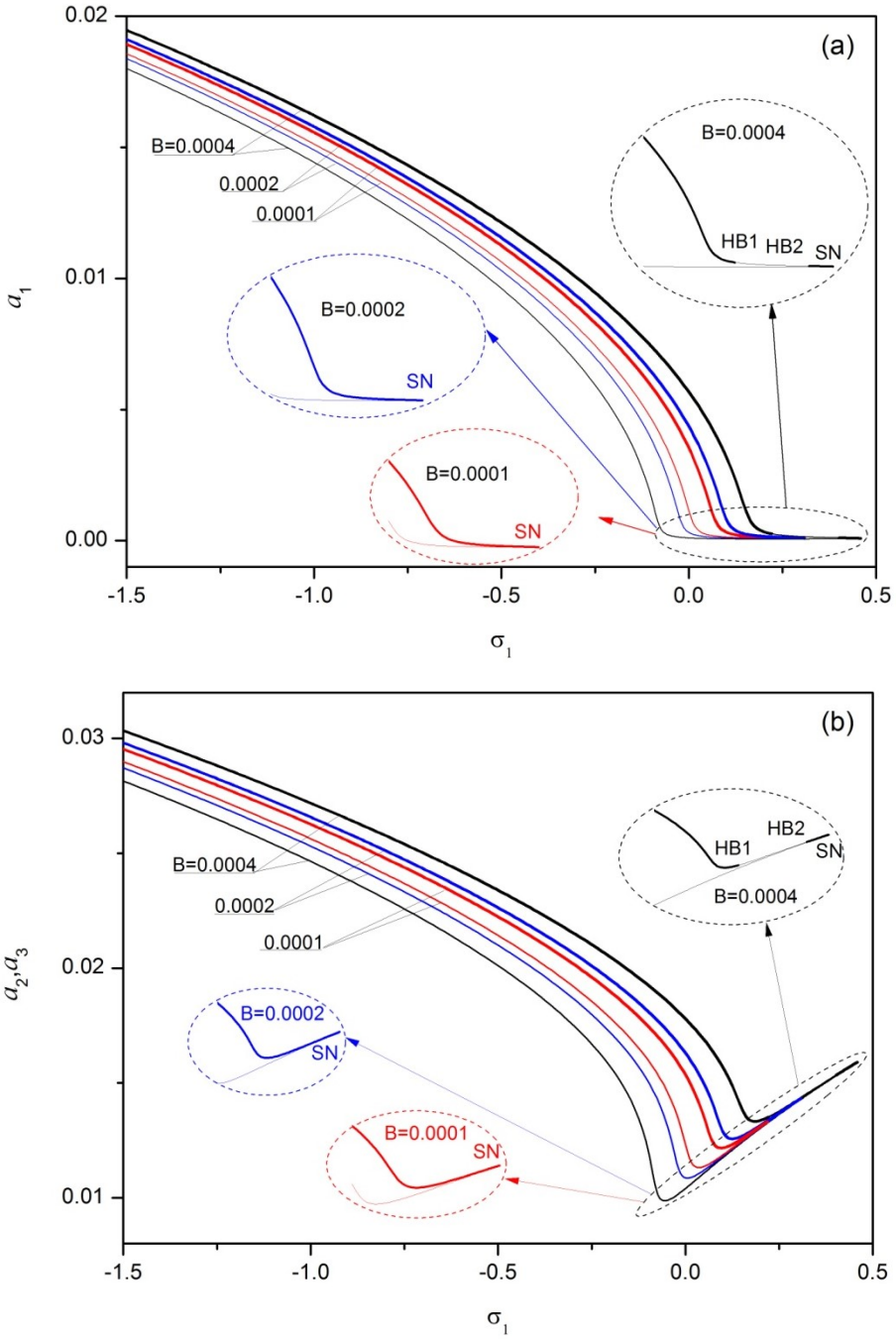

Fig.10 Frequency-response curves of modal amplitudes a_1, a_2 and a_3 to different excitation amplitudes with $\sigma_2=\sigma_3=-0.14$: (a) for cables and (b) for shallow arch.

Fig.11 shows modal response amplitudes of cables and shallow arch for increasing excitation amplitude with $\sigma_2=\sigma_3=-0.14$. Here the focus is on the exploration of dynamics of the system for

$\sigma_1<0$ since that the response amplitudes are considerably greater than those for $\sigma_1>0$. It is noted that the response not only for cables but for shallow arch increase with increasing of excitation amplitude with a constant excitation frequency. Similarly, for a constant excitation amplitude, the response of the system increases with decreasing of excitation frequency, which is also shown in Fig. 10.

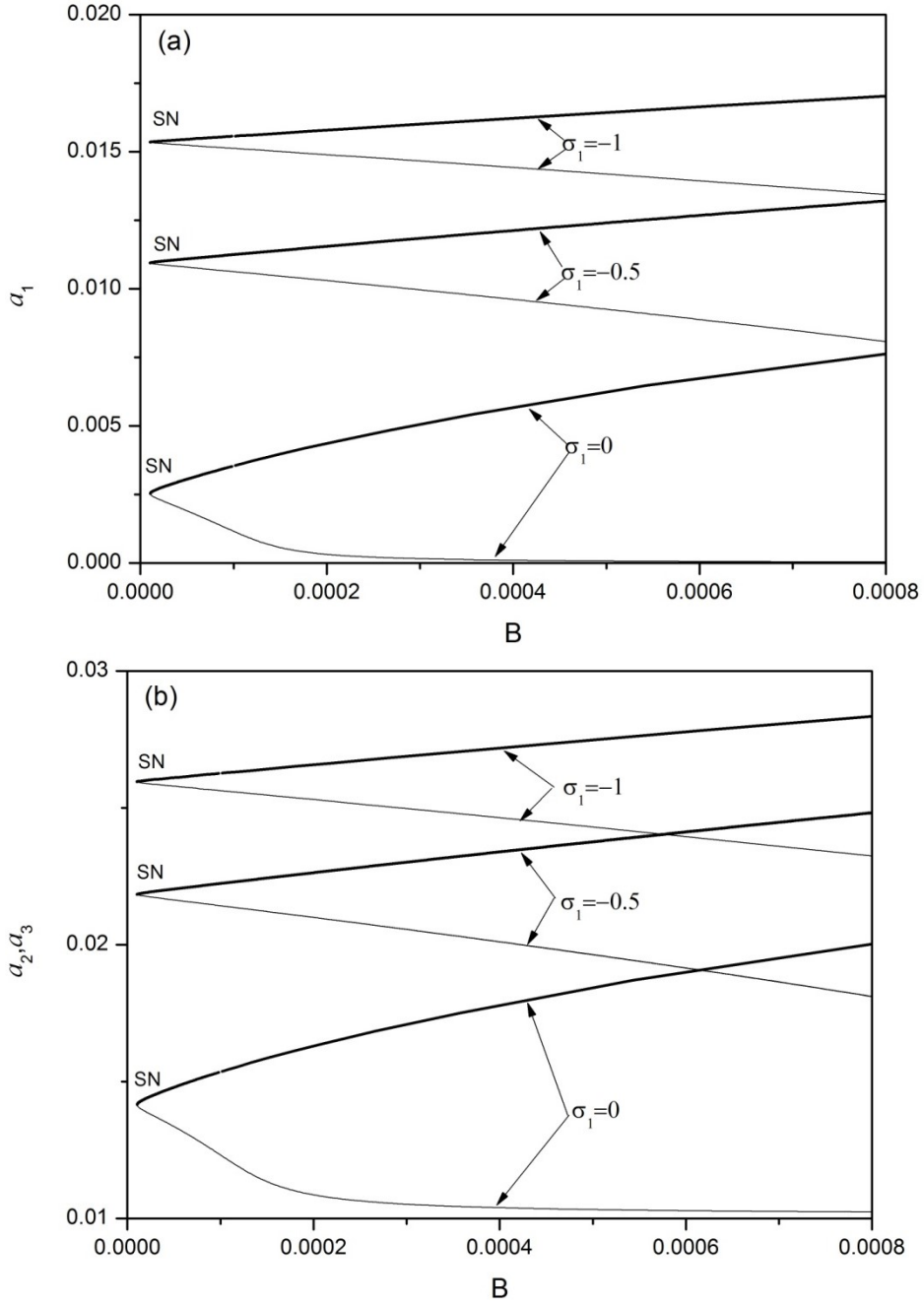

Fig.11 Modal amplitudes a_1, a_2 and a_3 for increasing excitation amplitude with $\sigma_2=\sigma_3=-0.14$: (a) for shallow arch and (b) for cables.

Fig.12 and Fig.13 show the influence of the parametric difference between two cables on the dynamics of the double-cable-stayed shallow arch system. Firstly, it is noted that the difference between a_2 and a_3 is almost ignorable when the difference between the two frequencies of cables is small, namely σ_2=-0.17 and σ_3=-0.5. However, the response of cable 2# is considerably greater than that of cable 1# when σ_2=-0.14 and σ_3=-0.99, which is also seen in Fig.13. Furthermore, as

can be seen from Fig.12, the type of bifurcation of both cables changes with increasing of the difference between the cables' frequencies. The Hopf bifurcation and saddle-node bifurcation are identified when the two cables are identical. The Hopf bifurcation vanishes when σ_2=-0.17 and σ_3=-0.5. And then, the saddle-node bifurcation vanishes and a Hopf bifurcation is identified again. Therefore, the difference between cables can change the dynamics of not only a cable but also the system. This is also shown in Fig.13. As can be noted that the number of equilibrium solutions of the system increases to four from two when σ_2=-0.14 and σ_3=-0.99.

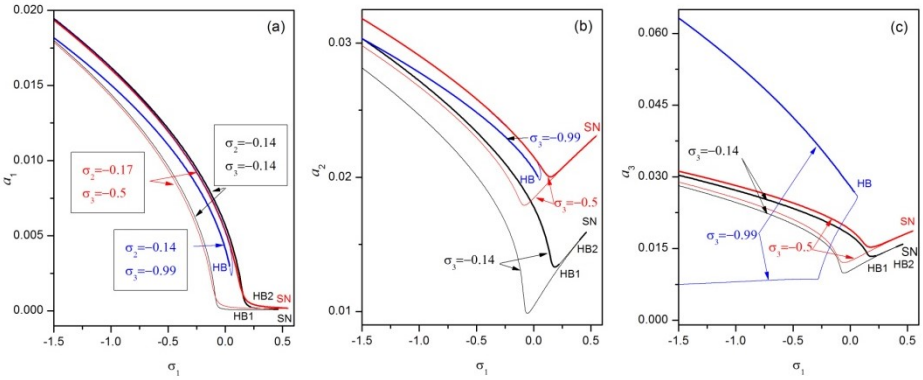

Fig.12 Frequency response curves of modal amplitudes a_1, a_2 and a_3 to excitation amplitude B=0.0004 with σ_2=-0.14: (a) for shallow arch, (b) and (c) for cables.

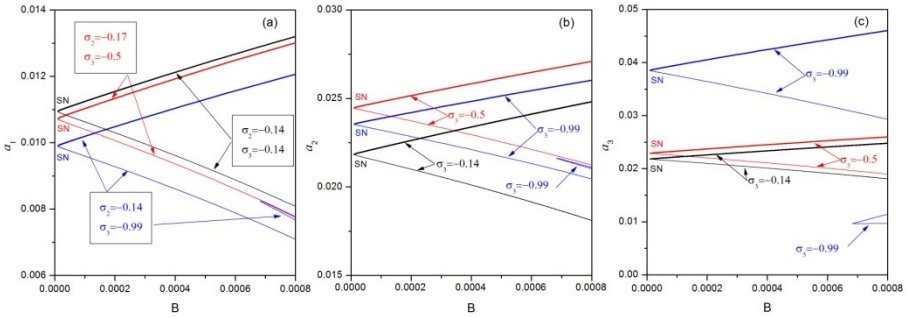

Fig.13 Modal amplitudes a_1, a_2 and a_3 for increasing excitation amplitude with σ_2=-0.14 : (a) for shallow arch, (b) and (c) for cables.

6. Conclusion

A novel nonlinear dynamic model, namely double-cable-stayed shallow arch model, of cable-stayed bridge has been established where the shallow arch is used to model the bridge deck with consideration of its initial geometric configuration. The nonlinear governing equations of the dynamic system were derived and solved. Comparisons between asymptotic and numerical integrations results of the discrete equations have been made. Response curves have been obtained by varying either the amplitude or the frequency of a symmetric horizontal harmonic forcing near primary and subharmonic external resonance. A rich behavior of the system associated with the existence of periodic motion, saddle-node bifurcation and Hopf bifurcation is deduced from the results presented. Especially, the following conclusion can be drawn from the results presented. Firstly, for the two identical cables, they may behave different motions even the identical initial conditions are given under external primary resonance. Secondly, for two different cables, the difference between them can change the dynamic behavior of not only a cable (local mode) but

also the system (global and hybrid mode).

Additionally, the novel double-cable-stayed shallow arch model can reveal practically the rich dynamic behavior of cable-stayed bridge. Although the 1:1:1 internal resonance between two cables and bridge deck has been discussed only, the richer dynamic behavior can be explored by this model in our following work, such as 1:2:1, 2:1:1 internal resonance between cables and bridge deck.

Acknowledgment

This study is funded by Supporting Program for Young Investigators, Hunan University. And it is also supported by National Science Foundation of China under Grant No.11572117 and No. 11502076. Interesting comments and criticism by the reviewers are also gratefully acknowledged.

References

Abdel-Ghaffar. A.M., Khalifa, M., 1991. Importance of cable vibration in dynamics of cable-stayed bridges. J. Eng. Mech. 117(11), 2571-89.

Arafat, H.N., Nayfeh, A.H., 2003. Non-linear responses of suspended cables to primary resonance excitations. J. Sound Vib. 266(2), 325-354

Bruno, D., Leonardi, A., 1997. Natural periods of long-span cable-stayed bridges. J. Bridge Eng. 2(3), 105-115.

Caetano, E., Cunha, A., Gattulli, V., Lepidi, M., 2008. Cable-deck dynamic interactions at the International Guadiana Bridge: on-site measurements and finite element modeling. Struct. Control Hlth. 15(3), 237-264.

Caetano, E., Cunha, A., Taylor, C.A., 2000. Investigation of dynamic cable-deck interaction in a physical model of a cable-stayed bridge. Part I: modal analysis. Earth. Eng. Struct. D. 29(4), 481-498

Cao, D.Q., Song, M.T., Zhu, W.D., Tucker, R.W., Wang, H.T., 2012.Modeling and analysis of the in-plane vibration of a complex cable-stayed bridge. J. Sound Vib. 331 (26), 5685-5714

Chang, C.C., Chang, T. Y. P., Zhang. Q. W., 2001. Ambient vibration of long-span cable-stayed bridge. J. Bridge Eng. 6(1), 46-53

Chen, L.Q., Zhang, Y.L., Zhang, G.C., Ding, H., 2014. Evolution of the double-jumping in pipes conveying fluid flowing at the supercritical speed. Int. J. Nonlin. Mech. 58(1), 11-21

Ding, H., Chen, L.Q., 2010. Galerkin methods for natural frequencies of high-speed axially moving beams. J. Sound Vib., 329(17), 3484-3494

Gattulli, V., Lepidi, M., 2007. Localization and veering in the dynamics of cable-stayed bridges. Comput. Struct. 85(21), 1661-1678.

Gattulli, V. , Lepidi, M. , Macdonald, J.H.G. , Taylor, C.A. , 2005。One-to-two global-local interaction in a cable-stayed beam observed through analytical, finite element and experimental models. Int. J. Nonlin. Mech. 40(4), 571-588.

Gattulli, V., Lepidi, M., 2003.Nonlinear interactions in the planar dynamics of cable-stayed beam. Int. J. Solids Struct. 40(18), 4729-4748

Gattulli, V., Morandini, M., Paolone, A., 2002. A parametric analytical model for non-linear

dynamics in cable-stayed beam. Earth. Eng. Struct. D. 31(6), 1281-1300.
Gimsing, N.J., Georgakis, C.T., 1983.Cable Supported Bridges. Wiley,
Guo, T., Kang, H., Wang, L., Zhao, Y., 2016. A boundary modulation formulation for cable's non-planar coupled dynamics under out-of-plane support motion. Arch. Appl. Mech. doi:10.1007/s00419-015-1058-8
Hagedorn, P., Schafer, B., 1980. On nonlinear free vibrations of an elastic cable. Int. J. Nonlin. Mech. 15(4-5), 333-339.
Irvine, H.M., 1981.Cable structures.The MIT Press, Cambridge Massachusetts, and London, England.
Kang, H., Zhao, Y. , Zhu, H. , Yi, Z., 2013. In-plane non-linear dynamics of the stay cables. Nonlinear Dynam. 73(3), 1385-1398
Kang, H.J., Zhao, Y.Y., Zhu, H.P., 2015.Linear and nonlinear dynamic of suspended cable considering bending stiffness. J. Vib. Control. 21(8), 1487-1505
Luongo, A., Rega, G., Vestroni, F. , 1984.Planar nonlinear free vibrations of an elastic cable. Int. J. Nonlin. Mech. 19(1), 39-52
Malhotra, N., Namachchivaya, N.S., 1997. Chaotic dynamics of shallow arch structures under 1:2 resonance. J. Eng. Mech. 123(6), 612-619
Mettler, E., 1962. Dynamic buckling. Flügge S., (Ed.), Handbook of Engineering Mechanics, McGraw-Hill, New York,
Nayfeh, A.H., Mook, D.T. , 1979. Nonlinear oscillations. Wiley, New York.
Ni, Y.Q., Ko, J.M., Zheng, G., 2002.Dynamic analysis of large-diameter sagged cables taking into account flexural rigidity. J. Sound Vib. 257(2), 301-19
Parker, T.S., Chua, L.O., 1989.Practical Numerical Algorithms for Chaotic Systems. Springer, New York.
Perkins, N.C., 1992. Modal interaction in the nonlinear response of elastic cables under parametric/external excitation. Int. J. Nonlin. Mech. 27(2), 233-54.
Pilipchuk, V. N., Ibrahim, R. A., 1999. Non-linear modal interactions in shallow suspended cables. J. Sound Vib. 227(1), 1-28.
Pilipchuk, V. N., Ibrahim, R. A., 1997. Strong nonlinear modal interaction in shallow suspended cables with oscillating ends. Chaos Soliton Fract. 8(8), 637-657.
Rega, G., 2004. Nonlinear vibrations of suspended cables—Part I: Modeling and analysis. Appl. Mech. Rev. 57(6), 443-478.
Rega, G., 2004. Nonlinear vibrations of suspended cables—part II: deterministic phenomena. Appl. Mech. Rev. 57(6), 479-514.
Ren, W.X., Peng, X.L., Lin, Y.Q., 2005.Experimental and analytical studies on dynamic characteristics of a large span cable-stayed bridge. Biomed. Res. Trace Ele. 27(4), 535-548.
Seydel, R., 2009.Practical Bifurcation and Stability Analysis. Springer, New York.
Srinil, N., Rega, G., 2008. Nonlinear longitudinal/transversal modal interactions in highly extensible suspended cables. J. Sound Vib. 310(1), 230-242
Starossek, U., 1994. Cable dynamics: A review. Struct. Eng. Int. 4(4), 171-176.
Triantafyllou, M. S., 1991. Dynamics of cables, towing cables and mooring systems. Shock Vib. Digest. 23(7), 3-8.
Warnitchai, P., Fujino, Y., Susumpow, T., 1995.A non-linear dynamic model for cables and its application to a cable-structure system. J. Sound Vib. 187(4), 695-712.

Warnitchai, P., Fujino, Y., Susumpow, T., 1995. A non-linear dynamic model for cables and its application to a cable – structure system. J. Sound Vib. 187(4), 695-712.
Wei, M.H., Xiao, Y.Q., Liu, H.T., Lin, K ., 2014.Nonlinear responses of a cable-beam coupled system under parametric and external excitations. Arch. Appl. Mech. 84 (2), 173-185.
Wei, M.H., Xiao, Y.Q., Liu, H.T. , 2012.Bifurcation and chaos of a cable – beam coupled system under simultaneous internal and external resonances. Nonlinear Dynam. 67(3), 1969-1984.
Wu, Q., Takahashi, K. , Okabayashi, T. , Nakamura, S., 2003. Response characteristics of local vibrations in stay cables on an existing cable-stayed bridge. J. Sound Vib. 261(3), 403-420
Yi, Z., Wang, L. , Kang, H., Tu, G., 2014.Modal interaction activations and nonlinear dynamic response of shallow arch with both ends vertically elastically constrained for two-to-one internal resonance. J. Sound Vib. 333(21), 5511-5524
Zhao, Y., Wang, L., 2006.On the symmetric modal interaction of the suspended cable: Three-to-one internal resonance. J. Sound Vib. 294(4), 1073-1093.
Zhou, Y., Chen, S., 2016.Framework of Nonlinear Dynamic Simulation of Long-Span Cable-Stayed Bridge and Traffic System Subjected to Cable-Loss Incidents. J. Struct. Eng. 142(3), doi:10.1061/(ASCE)ST.1943-541X.0001440

Appendix A

Firstly, in order to simplify the expression of Galerkin integral coefficients of Eqs. (18)-(20), here we introduce the following integrals

$$d_{mm}=\int_0^1 y'_m\varphi'_m\mathrm{d}x_m,\ d_{33}=\int_0^1 y'(s)\phi'(s)\mathrm{d}s,\ d_{0m}=\int_0^1 \varphi'_m(x_m)\mathrm{d}x_m,\ d_{m0}=\int_0^1 y'_m\mathrm{d}x_m,$$

$$f_{mm}=\int_0^1 y''_m\varphi_m\mathrm{d}x_m,\ h_{mm}=\int_0^1 \varphi_m\varphi''_m\mathrm{d}x_m,\ l_{mm}=\int_0^1 \varphi'_m\varphi'_m\mathrm{d}x_m,\ s_{mm}=\int_0^1 x_m\varphi_m\mathrm{d}x_m,$$

$$r_{33}=\int_0^1 \phi^{(4)}\phi\mathrm{d}s,\ \Gamma_{mm}=1\Big/\int_0^1 \varphi_m\varphi_m\mathrm{d}x_m,\ (m=0,1,2,3),$$

where m=0 represents there is no corresponding term, and φ_m and y_m denote the mode shapes and initial configurations of cables and shallow arch, respectively, and $\varphi_3=\phi$ and $y_3=y$.

Then, the coefficients in Eqs. (18)-(20) are given as follows:

$$b_{11}=\omega_a^2=\Gamma_{33}(r_{33}-\eta d_{33}f_{33})/\beta^4-\frac{1}{2}\Gamma_{33}\sum_{j=1}^{2}d_{j0}K_j\phi^2(s_j)\sin 2\theta_j+\Gamma_{33}\sum_{j=1}^{2}\gamma_jK_j\phi^2(s_j)\sin^2\theta_j,$$

$$b_{12}=-\Gamma_{33}B\eta h_{33}/\beta^4,\ b_{13}=-\frac{\Gamma_{33}\eta(2d_{33}h_{33}+f_{33}l_{33})}{2\beta^4}-\frac{\Gamma_{33}}{2}\sum_{j=1}^{2}K_j\phi^3(s_j)\cos^2\theta_j\sin\theta_j,$$

$$b_{14}=-\eta\Gamma_{33}l_{33}h_{33}/(2\beta^4),\ b_{15}=-\Gamma_{33}K_1\phi(s_1)d_{11}\sin\theta_1,\ b_{16}=-\tfrac{1}{2}\Gamma_{33}K_1\phi^2(s_1)d_{01}\sin 2\theta_1,$$

$$b_{17}=-\tfrac{1}{2}\Gamma_{33}K_1\phi(s_1)l_{11}\sin\theta_1,\ b_{18}=-\Gamma_{33}K_2\phi(s_2)d_{22}\sin\theta_2,\ b_{19}=-\tfrac{1}{2}\Gamma_{33}K_2\phi^2(s_2)d_{02}\sin 2\theta_2,$$

$$b_{110}=-\tfrac{1}{2}\Gamma_{33}K_2\phi(s_2)l_{02}\sin\theta_2,\ b_{111}=-\Gamma_{33}f_{33}B\eta/\beta^4,\ b_{21}=\mu_1\Gamma_{11}s_{11}\phi(s_1)\cos\theta_1,$$

$$b_{22}=\Gamma_{11}s_{11}\phi(s_1)\cos\theta_1,\ b_{23}=-\lambda_1\Gamma_{11}f_{11}\phi(s_1)(d_{10}\cos\theta_1+\gamma_1\sin\theta_1)/\beta_1^2,$$

$b_{24} = -\lambda_1 \Gamma_{11} f_{11} \phi^2(s_1) \cos^2\theta_1 / (2\beta_1^2)$, $b_{25} = \omega_b^2 = -\Gamma_{11}(\lambda_1 d_{11} f_{11} + h_{11})/\beta_1^2$,

$b_{26} = -\lambda_1 \phi(s_1) \Gamma_{11}(d_{10} h_{11} \cos\theta_1 + f_{11} d_{01} l_{10} \cos\theta_1 + \gamma_1 h_{11} \sin\theta_1)/\beta_1^2$,

$b_{27} = -\lambda_1 \Gamma_{11} h_{11} \phi^2(s_1) \cos^2\theta_1 / (2\beta_1^2)$, $b_{28} = -\lambda_1 \Gamma_{11}(2 d_{11} h_{11} + f_{11} l_{11})/(2\beta_1^2)$,

$b_{29} = -\lambda_1 \phi(s_1) \Gamma_{11} d_{01} h_{11} \cos\theta_1 / \beta_1^2$, $b_{210} = -\lambda_1 \Gamma_{11} l_{11} h_{11} / (2\beta_1^2)$, $b_{31} = \mu_2 \Gamma_{22} s_{22} \phi(s_2) \cos\theta_2$,

$b_{32} = \Gamma_{22} s_{22} \phi(s_2) \cos\theta_2$, $b_{33} = -\lambda_2 \Gamma_{22} f_{22} \phi(s_2)(d_{20} \cos\theta_2 + \gamma_2 \sin\theta_2)/\beta_2^2$,

$b_{34} = -\lambda_2 \Gamma_{22} f_{22} \phi^2(s_2) \cos^2\theta_2 / (2\beta_2^2)$, $b_{35} = \omega_c^2 = -\Gamma_{22}(\lambda_2 d_{22} f_{22} + h_{22})/\beta_2^2$,

$b_{36} = -\lambda_2 \phi(s_2) \Gamma_{22}(d_{20} h_{22} \cos\theta_2 + f_{22} d_{02} l_{10} \cos\theta_2 + \gamma_2 h_{22} \sin\theta_2)/\beta_2^2$,

$b_{37} = -\lambda_2 \Gamma_{22} h_{22} \phi^2(s_2) \cos^2\theta_2 / (2\beta_2^2)$, $b_{38} = -\lambda_2 \Gamma_{22}(2 d_{22} h_{22} + f_{22} l_{22})/(2\beta_2^2)$,

$b_{39} = -\lambda_2 \phi(s_2) \Gamma_{22} d_{02} h_{22} \cos\theta_2 / \beta_2^2$, $b_{310} = -\lambda_2 \Gamma_{22} l_{22} h_{22} / (2\beta_2^2)$.

Appendix B

The coefficients of Equations (41) - (43) are defined as follows:

$$\Gamma_1^{\mathrm{a}} = \frac{b_{15} b_{23}}{\omega_b^2 - \omega_a^2} - \frac{b_{18} b_{33}}{\omega_a^2 - \omega_c^2}, \quad \Gamma_2^{\mathrm{a}} = \frac{10 b_{13}^2}{3\omega_a^2} - 3 b_{14} + \frac{2 b_{16} b_{24}}{\omega_b^2} - \frac{b_{16} b_{24}}{4\omega_a^2 - \omega_b^2} + \frac{2 b_{19} b_{34}}{\omega_c^2} - \frac{b_{19} b_{34}}{4\omega_a^2 - \omega_c^2},$$

$$\Gamma_3^{\mathrm{a}} = \frac{2 b_{13} b_{16}}{2\omega_a \omega_b - \omega_b^2} - \frac{b_{13} b_{16}}{3\omega_a^2} - \frac{b_{16} b_{26}}{\omega_a^2 - 2\omega_a \omega_b} - \frac{2 b_{17} b_{24}}{4\omega_a^2 - \omega_b^2},$$

$$\Gamma_4^{\mathrm{a}} = \frac{2 b_{13} b_{16}}{\omega_a^2} + \frac{4 b_{17} b_{24}}{\omega_b^2} - \frac{2 b_{16} b_{26}}{\omega_a^2 - 4\omega_b^2} + \frac{4 b_{13} b_{16}}{4\omega_a^2 - \omega_b^2},$$

$$\Gamma_5^{\mathrm{a}} = \frac{b_{16}^2}{2\omega_a \omega_b - \omega_b^2} - \frac{b_{28} b_{16}}{3\omega_b^2} - \frac{2 b_{17} b_{26}}{\omega_a^2 - 2\omega_a \omega_b} + \frac{2 b_{17} b_{13}}{\omega_a^2 - 4\omega_b^2}$$

$$\Gamma_6^{\mathrm{a}} = \frac{2 b_{13} b_{19}}{\omega_a^2} + \frac{4 b_{110} b_{34}}{\omega_c^2} - \frac{2 b_{19} b_{36}}{\omega_a^2 - 4\omega_c^2} + \frac{4 b_{13} b_{19}}{4\omega_a^2 - \omega_c^2}, \quad \Gamma_7^{\mathrm{a}} = \frac{b_{16} b_{19}}{2\omega_a \omega_b - \omega_b^2} + \frac{b_{16} b_{19}}{2\omega_a \omega_c - \omega_c^2},$$

$$\Gamma_8^{\mathrm{a}} = \frac{b_{19}^2}{2\omega_a \omega_c - \omega_c^2} - \frac{2 b_{110} b_{36}}{\omega_a^2 - 2\omega_a \omega_c} - \frac{b_{19} b_{38}}{3\omega_c^2} - \frac{2 b_{110} b_{13}}{4\omega_c^2 - \omega_a^2},$$

$$\Gamma_9^{\mathrm{a}} = \frac{2 b_{13} b_{19}}{2\omega_a \omega_c - \omega_c^2} - \frac{b_{13} b_{19}}{3\omega_a^2} - \frac{b_{19} b_{36}}{\omega_a^2 - 2\omega_a \omega_c} - \frac{2 b_{110} b_{34}}{4\omega_a^2 - \omega_c^2},$$

$$\Gamma_{10}^{\mathrm{a}} = \frac{2 b_{110} b_{19}}{\omega_a^2} + \frac{10 b_{110} b_{38}}{3\omega_c^2} + \frac{b_{110} b_{19}}{\omega_a^2 - 4\omega_c^2}, \quad \Gamma_{11}^{\mathrm{a}} = \frac{4 b_{13} b_{17}}{\omega_a^2} + \frac{2 b_{16} b_{28}}{\omega_b^2} - \frac{4 b_{17} b_{26}}{\omega_a^2 - 4\omega_b^2} + \frac{2 b_{16}^2}{4\omega_a^2 - \omega_b^2},$$

$$\Gamma_{12}^{\mathrm{a}}=\frac{2b_{16}b_{17}}{\omega_a^2}+\frac{10b_{17}b_{28}}{3\omega_b^2}+\frac{b_{17}b_{16}}{\omega_a^2-4\omega_b^2},\ \Gamma_{13}^{\mathrm{a}}=\frac{b_{110}b_{16}}{4\omega_c^2-\omega_a^2},\ \Gamma_{14}^{\mathrm{a}}=\frac{2b_{19}b_{17}}{\omega_a^2},$$

$$\Gamma_{15}^{\mathrm{a}}=\frac{4b_{110}b_{13}}{\omega_a^2}+\frac{2b_{19}b_{38}}{\omega_c^2},\ \Gamma_{16}^{\mathrm{a}}=\frac{2b_{110}b_{16}}{\omega_a^2},\ \Gamma_{17}^{\mathrm{a}}=\frac{b_{16}b_{19}}{2\omega_a\omega_b-\omega_b^2}-\frac{b_{16}b_{19}}{2\omega_a\omega_c+\omega_c^2},$$

$$\Gamma_{18}^{\mathrm{a}}=\frac{2b_{19}^2}{4\omega_a^2-\omega_c^2}-\frac{4b_{110}b_{36}}{\omega_a^2-4\omega_c^2},\ \Gamma_{19}^{\mathrm{a}}=\frac{b_{16}b_{19}}{2\omega_a\omega_c-\omega_c^2}-\frac{b_{16}b_{19}}{2\omega_a\omega_b+\omega_b^2},\ \Gamma_{20}^{\mathrm{a}}=\frac{b_{17}b_{19}}{\omega_a^2-4\omega_b^2};$$

$$\Gamma_{1}^{\mathrm{b}}=\frac{b_{15}b_{23}}{\omega_a^2-\omega_b^2},\ \Gamma_{2}^{\mathrm{b}}=\frac{b_{18}b_{23}}{\omega_a^2-\omega_c^2},\ \Gamma_{3}^{\mathrm{b}}=\frac{10b_{13}b_{24}}{3\omega_a^2}+\frac{2b_{24}b_{26}}{\omega_b^2}-\frac{b_{24}b_{26}}{4\omega_a^2-\omega_b^2},$$

$$\Gamma_{4}^{\mathrm{b}}=\frac{2b_{13}b_{26}}{\omega_a^2}-2b_{27}+\frac{4b_{24}b_{28}}{\omega_b^2}-\frac{2b_{26}^2}{\omega_a^2-4\omega_b^2}+\frac{4b_{16}b_{24}}{4\omega_a^2-\omega_b^2},$$

$$\Gamma_{5}^{\mathrm{b}}=\frac{2b_{17}b_{24}}{\omega_a^2-4\omega_b^2}-\frac{b_{26}b_{28}}{3\omega_b^2}-b_{29}-\frac{2b_{26}b_{28}}{\omega_a^2-2\omega_a\omega_b}-\frac{2b_{16}b_{26}}{\omega_b^2-2\omega_a\omega_b},\ \Gamma_{6}^{\mathrm{b}}=\frac{4b_{19}b_{24}}{4\omega_a^2-\omega_c^2},$$

$$\Gamma_{7}^{\mathrm{b}}=\frac{b_{19}b_{26}}{2\omega_a\omega_c-\omega_c^2},\ \Gamma_{8}^{\mathrm{b}}=\frac{2b_{110}b_{24}}{\omega_a^2-4\omega_c^2},$$

$$\Gamma_{9}^{\mathrm{b}}=\frac{2b_{16}b_{24}}{2\omega_a\omega_b-\omega_b^2}-\frac{b_{13}b_{26}}{3\omega_a^2}-b_{27}-\frac{b_{26}^2}{\omega_a^2-2\omega_a\omega_b}-\frac{2b_{24}b_{28}}{4\omega_a^2-\omega_b^2},\ \Gamma_{10}^{\mathrm{b}}=\frac{2b_{19}b_{24}}{2\omega_a\omega_c-\omega_c^2},$$

$$\Gamma_{11}^{\mathrm{b}}=\frac{4b_{17}b_{24}}{\omega_a^2}-2b_{29}+\frac{2b_{26}b_{28}}{\omega_b^2}-\frac{4b_{26}b_{28}}{\omega_a^2-4\omega_b^2}+\frac{2b_{16}b_{26}}{4\omega_a^2-\omega_b^2},$$

$$\Gamma_{12}^{\mathrm{b}}=\frac{2b_{17}b_{26}}{\omega_a^2}-3b_{210}+\frac{10b_{28}^2}{3\omega_b^2}+\frac{b_{17}b_{26}}{\omega_a^2-4\omega_b^2},\ \Gamma_{13}^{\mathrm{b}}=-\frac{b_{19}b_{26}}{2\omega_a\omega_c+\omega_c^2},\ \Gamma_{14}^{\mathrm{b}}=\frac{b_{110}b_{26}}{\omega_a^2-4\omega_c^2},$$

$$\Gamma_{15}^{\mathrm{b}}=\frac{b_{19}b_{26}}{2\omega_a\omega_c-\omega_c^2},\ \Gamma_{16}^{\mathrm{b}}=\frac{4b_{110}b_{24}}{\omega_a^2},\ \Gamma_{17}^{\mathrm{b}}=\frac{2b_{110}b_{26}}{\omega_a^2},$$

$$\Gamma_{1}^{\mathrm{c}}=\frac{b_{18}b_{33}}{\omega_a^2-\omega_c^2},\ \Gamma_{2}^{\mathrm{c}}=\frac{b_{15}b_{33}}{\omega_a^2-\omega_b^2},\ \Gamma_{3}^{\mathrm{c}}=\frac{10b_{13}b_{34}}{3\omega_a^2}+\frac{2b_{34}b_{36}}{\omega_c^2}-\frac{b_{34}b_{36}}{4\omega_a^2-\omega_c^2},$$

$$\Gamma_{4}^{\mathrm{c}}=\frac{2b_{13}b_{36}}{\omega_a^2}-2b_{37}+\frac{4b_{34}b_{38}}{\omega_c^2}-\frac{2b_{36}^2}{\omega_a^2-4\omega_c^2}+\frac{4b_{19}b_{34}}{4\omega_a^2-\omega_c^2},$$

$$\Gamma_{5}^{\mathrm{c}}=\frac{b_{19}b_{36}}{2\omega_a\omega_c-\omega_c^2}-\frac{b_{36}b_{38}}{3\omega_c^2}-b_{39}-\frac{2b_{36}b_{38}}{\omega_a^2-2\omega_a\omega_c}+\frac{2b_{110}b_{34}}{\omega_a^2-4\omega_c^2},\ \Gamma_{6}^{\mathrm{c}}=\frac{4b_{16}b_{34}}{4\omega_a^2-\omega_b^2},$$

$$\Gamma_{7}^{\mathrm{c}}=\frac{b_{16}b_{36}}{2\omega_a\omega_b-\omega_b^2},\ \Gamma_{8}^{\mathrm{c}}=\frac{2b_{17}b_{34}}{\omega_a^2-4\omega_b^2},$$

$$\Gamma_9^c = \frac{2b_{19}b_{34}}{2\omega_a\omega_c - \omega_c^2} - \frac{b_{13}b_{36}}{3\omega_a^2} - b_{37} - \frac{b_{36}^2}{\omega_a^2 - 2\omega_a\omega_c} - \frac{2b_{34}b_{38}}{4\omega_a^2 - \omega_c^2}, \quad \Gamma_{10}^c = \frac{2b_{16}b_{34}}{2\omega_a\omega_b - \omega_b^2},$$

$$\Gamma_{11}^c = \frac{4b_{110}b_{34}}{\omega_a^2} - 2b_{39} + \frac{2b_{36}b_{38}}{\omega_c^2} - \frac{4b_{36}b_{38}}{\omega_a^2 - 4\omega_c^2} + \frac{2b_{19}b_{36}}{4\omega_a^2 - \omega_c^2},$$

$$\Gamma_{12}^c = \frac{2b_{110}b_{36}}{\omega_a^2} - 3b_{310} + \frac{10b_{38}^2}{3\omega_c^2} + \frac{b_{110}b_{36}}{\omega_a^2 - 4\omega_c^2}, \quad \Gamma_{13}^c = -\frac{b_{16}b_{36}}{2\omega_a\omega_b + \omega_b^2}, \quad \Gamma_{14}^c = \frac{b_{17}b_{36}}{\omega_a^2 - 4\omega_b^2},$$

$$\Gamma_{15}^c = \frac{b_{16}b_{36}}{2\omega_a\omega_b - \omega_b^2}, \quad \Gamma_{16}^c = \frac{4b_{17}b_{34}}{\omega_a^2}, \quad \Gamma_{17}^c = \frac{2b_{17}b_{36}}{\omega_a^2}.$$